AMERICAN SOCIETY FOR MICROBIOLOGY | Journal of Bacteriology®

RESEARCH ARTICLE

Elevated Levels of the *Escherichia coli nrdAB*-Encoded Ribonucleotide Reductase Counteract the Toxicity Caused by an Increased Abundance of the β Clamp

Vignesh M. P. Babu,[a]* Caleb Homiski,[a] Michelle K. Scotland,[a] Sundari Chodavarapu,[b]§ Jon M. Kaguni,[b] Mark D. Sutton[a]

[a]Department of Biochemistry, Jacobs School of Medicine and Biomedical Sciences, University at Buffalo, State University of New York, Buffalo, New York, USA
[b]Department of Biochemistry and Molecular Biology, Michigan State University, East Lansing, Michigan, USA

Caleb Homiski and Michelle K. Scotland contributed equally to this work. Author order was determined alphabetically.

ABSTRACT Expression of the *Escherichia coli dnaN*-encoded β clamp at ≥10-fold higher than chromosomally expressed levels impedes growth by interfering with DNA replication. A mutant clamp (β^{E202K} bearing a glutamic acid-to-lysine substitution at residue 202) binds to DNA polymerase III (Pol III) with higher affinity than the wild-type clamp, suggesting that its failure to impede growth is independent of its ability to sequester Pol III away from the replication fork. Our results demonstrate that the *dnaN*^{E202K} strain underinitiates DNA replication due to insufficient levels of DnaA-ATP and expresses several DnaA-regulated genes at altered levels, including *nrdAB*, that encode the class 1a ribonucleotide reductase (RNR). Elevated expression of *nrdAB* was dependent on *hda* function. As the β clamp-Hda complex regulates the activity of DnaA by stimulating its intrinsic ATPase activity, this finding suggests that the *dnaN*^{E202K} allele supports an elevated level of Hda activity *in vivo* compared with the wild-type strain. In contrast, using an *in vitro* assay reconstituted with purified components the β^{E202K} and wild-type clamp proteins supported comparable levels of Hda activity. Nevertheless, co-overexpression of the *nrdAB*-encoded RNR relieved the growth defect caused by elevated levels of the β clamp. These results support a model in which increased cellular levels of DNA precursors relieve the ability of elevated β clamp levels to impede growth and suggest either that multiple effects stemming from the *dnaN*^{E202K} mutation contribute to elevated *nrdAB* levels or that Hda plays a noncatalytic role in regulating DnaA-ATP by sequestering it to reduce its availability.

IMPORTANCE DnaA bound to ATP acts in initiation of DNA replication and regulates the expression of several genes whose products act in DNA metabolism. The state of the ATP bound to DnaA is regulated in part by the β clamp-Hda complex. The *dnaN*^{E202K} allele was identified by virtue of its inability to impede growth when expressed ≥10-fold higher than chromosomally expressed levels. While the *dnaN*^{E202K} strain exhibits several phenotypes consistent with heightened Hda activity, the wild-type and β^{E202K} clamp proteins support equivalent levels of Hda activity *in vitro*. Taken together, these results suggest that β^{E202K}-Hda plays a noncatalytic role in regulating DnaA-ATP. This, as well as alternative models, is discussed.

KEYWORDS DNA polymerase, DNA replication, DnaA, fidelity, Hda, initiation, ribonucleotide reductase, sliding clamp, protein-protein interactions, transcriptional regulation

The *Escherichia coli* β clamp plays pivotal roles in DNA replication, DNA repair, and DNA damage tolerance (1–4). As a homodimer, it has a ring-shaped structure with a central hole that can encircle double-stranded (ds) DNA (5, 6). Once loaded onto DNA by the DnaX clamp loader complex, the β clamp can interact with several partner

Citation Babu VMP, Homiski C, Scotland MK, Chodavarapu S, Kaguni JM, Sutton MD. 2021. Elevated levels of the *Escherichia coli nrdAB*-encoded ribonucleotide reductase counteract the toxicity caused by an increased abundance of the β clamp. J Bacteriol 203:e00304-21. https://doi.org/10.1128/JB.00304-21.

Editor Thomas J. Silhavy, Princeton University

Copyright © 2021 American Society for Microbiology. All Rights Reserved.

Address correspondence to Mark D. Sutton, mdsutton@buffalo.edu.

*Present address: Vignesh M. P. Babu, Department of Biology, Massachusetts Institute of Technology, Cambridge, Massachusetts, USA.

§Present address: Sundari Chodavarapu, Nivagen Pharmaceuticals Inc, Davis, California.

For a companion article on this topic, see https://doi.org/10.1128/JB.00303-21.

Received 2 June 2021
Accepted 11 September 2021
Accepted manuscript posted online 20 September 2021
Published 5 November 2021

Downloaded from https://journals.asm.org/journal/jb on 24 January 2022 by 35.10.240.139.

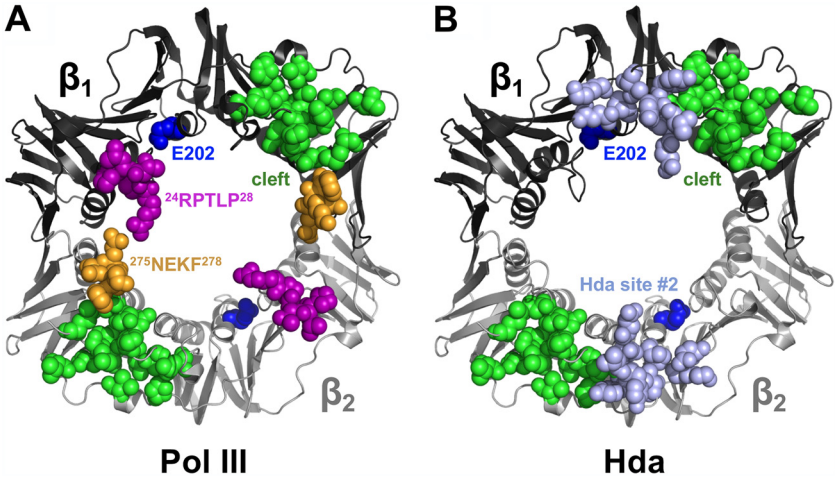

FIG 1 Location of residue E202 in the β clamp. (A) The location of residue E202 (blue) is represented on the X-ray crystal structure of the β clamp (PDB ID 3BEP). Clamp surfaces that interact with Pol III include the hydrophobic cleft (green) and residues ^{24}RPTLP^{28} (purple) and ^{275}NEKF^{278} (orange) that are located within respective solvent exposed loops. (B) Residue E202 (blue) is represented relative to two surfaces of the clamp that interact with Hda, including the cleft (green) and residues E50, Q149, V151, Y153, Y154, N156, P196, K235, and V237 (light blue). These images were generated using PyMOL 2.4.0.

proteins to tether them to the DNA for their respective functions (reviewed in reference 7). The partners include the five *E. coli* DNA polymerases (Pols) (2, 8, 9), DNA ligase (2), the chromosomal positioning protein CrfC (10), Hda protein that, together with the β clamp, regulates the activity of DnaA by stimulating the hydrolysis of ATP bound to DnaA (11), UmuD complexed with UmuC of Pol V ($UmuD_2C$) that is proposed to act in a primitive cell cycle checkpoint control (8), and MutS and MutL that act in mismatch repair (2, 12). In addition, during clamp loading and unloading from DNA, the β clamp interacts with the DnaX complex via the δ subunit of the complex.

Most clamp partners possess a pentameric or hexameric hydrophobic sequence called a clamp binding motif (CBM) that inserts into a hydrophobic cleft located between subdomains 2 and 3 of each clamp protomer (Fig. 1A) (13); a molecular understanding of how the β clamp interacts with these proteins is incomplete but is best understood for DNA polymerase III holoenzyme (Pol III HE), which is responsible for the majority of DNA replication. As an asymmetric dimer at the replication fork, it is comprised of 2 Pol III core complexes (Pol III$\alpha\varepsilon\theta$), 2 homodimeric β clamps that act to tether Pol III to the DNA, and the multisubunit ATP-dependent DnaX clamp loader ($\tau_2\gamma\delta\delta'\psi\chi$) complex (14, 15). Pol III interacts via its α (catalytic) and ε (proofreading) subunits with the β clamp (16–18). Other studies show that the affinity of the β clamp for Pol IIIα is influenced by DNA (19, 20). Based on the cryo-EM structure of the β clamp-Pol IIIα-Pol IIIε-DnaXτ_c complex (19), Pol IIIα contacts the β cleft independently of DNA. In the presence of primed DNA, Pol IIIα forms additional contacts with residues Arg^{24}-Pro^{28} and Asn^{275}-Phe^{278} of the β clamp (Fig. 1A).

Expression of the *E. coli* β clamp at $\geq$10-fold higher than chromosomally expressed levels severely impedes growth by blocking DNA replication (21). We previously described the identification of eight mutant β clamps that failed to inhibit growth when their expression was elevated (22, 23). Several of these mutants, which bear separate respective amino acid substitutions, were impaired for physical interactions with the catalytic subunit of Pol III (Pol IIIα) (24) and were deficient for stimulating Pol III replication *in vitro* (25). Their biochemical characterization supports a model in which elevated levels of the β clamp sequester Pol III, providing one explanation for why elevated cellular abundance of the β clamp impedes growth (25). However, a mutant clamp protein bearing a glutamic acid-to-lysine substitution at residue 202 (β^{E202K}; see

Downloaded from https://journals.asm.org/journal/jb on 24 January 2022 by 35.10.240.139.

Fig. 1A) displayed increased affinity for Pol IIIα and Pol III core (25). This finding is inconsistent with an elevated cellular abundance of β^{E202K} failing to sequester Pol III and suggests an alternate mechanism that permits bacterial growth under otherwise toxic conditions.

Studies show that the β clamp assembled on dsDNA and complexed with Hda and DnaA stimulates DnaA's intrinsic ATPase activity to convert DnaA-ATP, which is active in replication initiation, to DnaA-ADP, which is less active (26). Because recent results suggest that the *dnaN*^{E202K} allele causes less frequent initiation (25), we considered whether β^{E202K} is defective in its ability to stimulate the Hda-dependent hydrolysis of ATP bound to DnaA, leading to a lower cellular ratio of DnaA-ATP to DnaA-ADP and reduced initiations. The work described herein supports this idea in which DnaA-ATP levels are limiting for initiation in the *dnaN*^{E202K} strain. We further demonstrate that the expression of several genes regulated by DnaA-ATP is altered in the *dnaN*^{E202K} strain compared with the *dnaN*$^{+}$ control. Of these genes, we found an ~2-fold increase of *nrdA* and *nrdB* transcripts, which is dependent on *hda* function. As *nrdAB* encodes the class 1a ribonucleotide reductase (RNR) responsible for the production of DNA precursors required for replication (27), elevated RNR presumably leads to increased intracellular nucleotide pools that apparently alleviate the growth arrest caused by an elevated cellular abundance of the β clamp. Because the wild-type clamp and β^{E202K} support equivalent levels of Hda activity *in vitro*, we suggest that Hda may play a noncatalytic role in regulating DnaA-ATP by sequestering it to effectively reduce its available concentration.

RESULTS

The *dnaN*^{E202K} strain underinitiates DNA replication. The *dnaN*^{E202K} strain displays a reduced *oriC*/*TerC* ratio, suggesting that it is impaired for initiation (25). As an independent method to confirm this result, we used flow cytometry to measure the DNA content per cell under conditions in which cells completed DNA replication but were unable to undergo cell division. Compared with the isogenic *dnaN*$^{+}$ strain, the *dnaN*^{E202K} mutant displayed a decreased DNA/cell mass ratio, suggesting less frequent initiation (Fig. 2A). Of interest, transcriptome sequencing (RNA-seq) experiments showed that *dnaA* transcript levels were ~1.2-fold higher in the *dnaN*^{E202K} strain than the isogenic *dnaN*$^{+}$ control (Table 1). Thus, the lower frequency of initiation in the *dnaA*^{E202K} mutant is not the result of reduced *dnaA* transcript levels. As a control in which *dnaA*$^{+}$ expression was induced via a plasmid (pDS596) encoding *dnaA*$^{+}$ and confirmed by quantitative PCR (qPCR) (Fig. 2B), we measured more frequent initiation in the *dnaN*$^{+}$ and *dnaN*^{E202K} strains. These findings support the view that insufficient DnaA-ATP is responsible for the underinitiation observed in the *dnaN*^{E202K} strain.

Multiple DnaA-regulated genes are expressed at altered levels in the *dnaN*^{E202K} mutant. A lower relative abundance of DnaA-ATP implicates the involvement of the Hda-β clamp complex, which may decrease the proportion of DnaA-ATP to DnaA-ADP, leading to underinitiation. Because the state of the adenine nucleotide bound to DnaA influences its ability to regulate the expression of many genes, we considered the possibility that their expression was altered in the *dnaN*^{E202K} mutant compared with a *dnaN*$^{+}$ strain. For *dnaAN* ((28, 29), in which *dnaN* is expressed from the *dnaA* promoters during exponential growth), *guaBA* (30), *rpoH* (31), *mioC* (32, 33), *uvrB* (34, 35), *proS* (33), *aldA* (36), *recN*, and *dinJ* (34), DnaA-ATP represses transcription. In contrast, DnaA-ATP stimulates transcription of *polA* (37), *fliC* (38, 39), and *glpD* (33). For the *nrdAB* operon, transcription is stimulated by a reduced DnaA-ATP/DnaA-ADP ratio (i.e., lower relative cellular concentration of DnaA-ATP) but is repressed by an elevated DnaA-ATP/DnaA-ADP ratio (40). We used RNA-seq to measure the transcript levels of the DnaA-regulated genes described above. Because most are regulated by one or more transcription factors, we did not expect large changes in their expression. We found that the transcript levels for all but three genes were changed, with 6 of the 16 DnaA-regulated genes in the *dnaN*^{E202K} strain being changed by at least ~50% compared with the wild-type control (Table 1). As controls, qPCR analysis of *dnaA* and *polA*

Downloaded from https://journals.asm.org/journal/jb on 24 January 2022 by 35.10.240.139.

A

Strain	*dnaN* allele	Plasmid	DnaA overexpression	DNA/cell	Cell mass	DNA/cell mass
VB001	*dnaN*$^{+}$	pBR322	–	1	1	1
VB001	*dnaN*$^{+}$	pDS596	+	1.32 (±0.04)	1.19 (±0.04)	1.11 (±0.04)
VB019	*dnaN*^{E202K}	pBR322	–	1.01 (±0.04)	1.25 (±0.04)	0.81 (±0.03)
VB019	*dnaN*^{E202K}	pDS596	+	1.38 (±0.05)	1.23 (±0.07)	1.12 (±0.04)

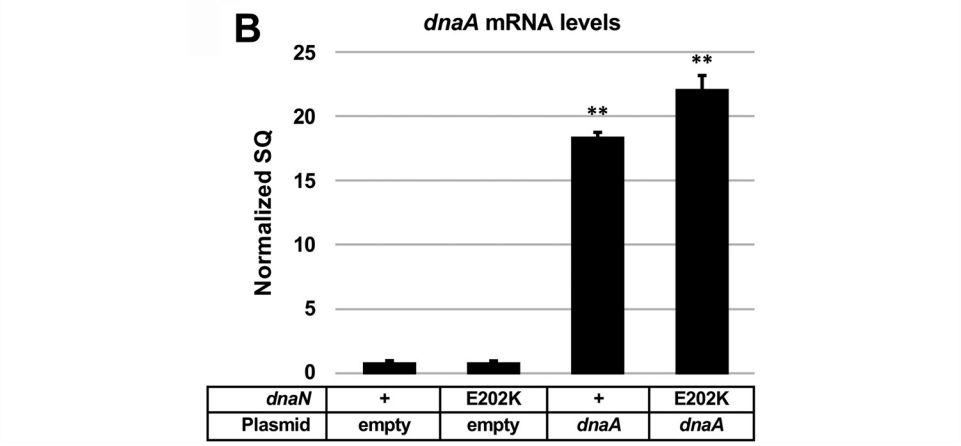

FIG 2 DnaA-ATP levels are limiting in the *dnaN*^{E202K} mutant. (A) Genome content after replication runout was measured by flow cytometry as described in Materials and Methods. The average cell mass was calculated as the average FITC (EMD Millipore) fluorescence. The average DNA/cell mass was calculated by dividing the average DNA content by the average cell mass. Results represent the average of 3 independent determinations ± SD. (B) The *dnaA* transcript levels in isogenic *dnaN*$^{+}$ (*E. coli* VB001) and *dnaN*^{E202K} (*E. coli* VB019) strains bearing either plasmid pBR322 or pDS596, which expresses DnaA from the *araBAD* promoter, were measured by qPCR. Values are the average of 3 determinations ± SD. **, $P \leq 0.001$ (Student's *t* test) relative to the *dnaN*$^{+}$ pBR322 empty plasmid control.

transcripts was performed with separate RNA preparations. The results confirm those obtained by RNA-seq analysis (Fig. 3).

Three genes (*mioC*, *recN*, and *glpD*) reported to be DnaA regulated were unchanged in the *dnaN*^{E202K} mutant compared with the *dnaN*$^{+}$ strain (Table 1). Perhaps DnaA does not regulate them under the growth conditions examined, and/or other transcription factors may affect their expression. With the exception of these genes and *aldA* and *dinJ* that are described below, the observed changes in transcript levels of the remainder are consistent with the *dnaN*^{E202K} strain containing a lower relative DnaA-ATP/DnaA-ADP ratio. These findings suggest that compared with the wild-type clamp, the β^{E202K} clamp complexed with Hda stimulates DnaA's ATPase activity, which leads to a lower DnaA-ATP/DnaA-ADP ratio.

Regarding *aldA*, its transcription is regulated by catabolite repression, anaerobiosis via ArcA, and FNR (41–45). Also, DnaA-ATP is reported to repress *aldA* expression (36). Thus, its transcript level should increase if the relative level of DnaA-ATP is lower in the *dnaN*^{E202K} mutant, yet it was reduced ~6.9-fold compared with the *dnaN*$^{+}$ control (Table 1). To explain this discrepancy, one or more of the other regulators may be responsible for the striking reduction in *aldA* transcript levels in the *dnaN*^{E202K} strain. For *dinJ*, its regulation by DnaA was measured by β-galactosidase activity using a promoter fusion to *lacZ* (34). A metabolically unstable *dinJ* transcript compared with a more stable *lacZ* transcript may account for the apparent inconsistency.

***hda* function is required for the elevated level of *nrdAB* expression in the *dnaN*^{E202K} mutant.** Based on RNA-seq analysis, *nrdA* and *nrdB* transcript levels were elevated ~2.3-fold and ~2.5-fold, respectively, in the *dnaN*^{E202K} mutant compared with the *dnaN*$^{+}$ control (Table 1). Likewise, qPCR and quantitative Western blot experiments showed that the *nrdB* transcript (Fig. 4A, compare bars 1 and 6) and protein levels in

Downloaded from https://journals.asm.org/journal/jb on 24 January 2022 by 35.10.240.139.

TABLE 1 Expression levels of DnaA-regulated genes in the *dnaN*^{E202K} strain[a]

Gene	Gene ID	Function[b]	Fold change relative to *dnaN*$^{+}$[c]
Genes repressed by an elevated DnaA-ATP/DnaA-ADP ratio			
dnaA	b3702	Replication initiator, transcriptional regulator	+1.21
dnaN	b3701	Processivity clamp	+1.31
nrdA[d]	b2234	α subunit of class 1a aerobic ribonucleotide reductase	+2.53
nrdB[d]	b2235	β subunit of class 1a aerobic ribonucleotide reductase	+2.25
guaA	b2507	GMP synthetase (guanine nucleotide biosynthesis)	+1.49
guaB	b2508	Inosine 5′-monophosphate dehydrogenase (guanine nucleotide biosynthesis)	+1.62
rpoH	b3461	RNA polymerase sigma 32 (sigma H) factor	+1.16
mioC	b3742	Flavoprotein involved in biotin synthesis, DnaA box upstream of *mioC* contributes to *oriC*-dependent replication	+1.03
uvrB	b0779	Nucleotide excision repair	+1.48
proS	b0194	Proline-tRNA ligase	+1.26
aldA	b1415	NAD^+-dependent dehydrogenase	−6.85
recN	b2616	Recombination	+1.06
dinJ	b0226	Antitoxin of YafQ toxin	−1.23
Genes activated by an elevated DnaA-ATP/DnaA-ADP ratio			
polA	b3863	Pol I, DNA replication and repair	−1.10
fliC	b1923	Flagellin	−1.30
glpD	b3426	Aerobic glycerol 3-phosphate dehydrogenase	−1.03

[a]Relative transcript levels were measured by RNA-seq.
[b]Gene function was defined by EcoCyc (https://ecocyc.org).
[c]A negative sign indicates a reduction in the transcript level relative to the isogenic *dnaN*$^{+}$ control, while a positive sign indicates an increase.
[d]The *nrdAB* genes are both repressed and activated by DnaA as a function of the DnaA-ATP/DnaA-ADP ratio (40).

the *dnaN*^{E202K} strain were ~2-fold elevated over the wild-type parent (Fig. 4B and C, compare lanes 1 and 6).

Because the effect of the *dnaN*^{E202K} mutation on *nrdAB* expression supports the idea that the mutant β^{E202K} clamp complexed to Hda results in a lower relative ratio of DnaA-ATP to DnaA-ADP, which leads to depressed *nrdAB* transcription, an elevated cellular abundance of Hda may have a similar effect. The experiments summarized in Fig. 5 confirm this expectation, showing an ~1.5-fold increase in the level of the *nrdB* transcript (Fig. 5A) and an ~1.7-fold increase in the steady-state level of the NrdB protein when Hda levels were elevated ~2-fold (Fig. 5B and C). Taken together, these results suggest that a decreased DnaA-ATP/DnaA-ADP ratio mediated by the β^{E202K} clamp-Hda complex, or by higher cellular levels of Hda, leads to elevated levels of NrdAB.

To obtain additional evidence of Hda's influence on *nrdAB* expression, we took advantage of a Δ*hda* strain. An issue to consider is that strains harboring a Δ*hda* mutation fail to grow at temperatures <37°C and grow poorly at temperatures ≥37°C due to more frequent initiation (46). At higher temperatures, Δ*hda* strains rapidly acquire suppressor mutations that both improve growth and also permit growth at temperatures lower than 37°C (46–48). To measure the effect of Hda on *nrdAB* expression, we used two genetically distinct Δ*hda* strains. For the reasons described below, they also carried the *dnaN*^{E202K} or *dnaN*$^{+}$ allele. One strain harbored the Δ*diaA* allele, which suppresses the growth defect caused by the Δ*hda* mutation. DiaA facilitates the binding of DnaA-ATP to *oriC* during replication initiation, whereas suppression occurs from less frequent initiation in cells lacking *diaA* and *hda* (49–51). The second Δ*hda* strain carried plasmid pRM100 that encodes DNA polymerase I (Pol I) and the N-terminal portion of YihG (YihG′), a lysophosphatidic acid acyltransferase that is upstream of *polA* and is expressed divergently (52). The plasmid suppresses the growth defect conferred by the Δ*hda* allele, suggesting that elevated levels of Pol I and/or YihG′ are responsible (51). Using a Δ*hda* mutant (suppressed by the Δ*diaA* mutation) that also carried the *dnaN*$^{+}$ allele, we measured a 2-fold decrease in *nrdB* transcripts compared with the isogenic *hda*$^{+}$ strain that also bore the Δ*diaA* and *dnaN*$^{+}$ alleles (Fig. 4A). In this set of experiments, the results

Downloaded from https://journals.asm.org/journal/jb on 24 January 2022 by 35.10.240.139.

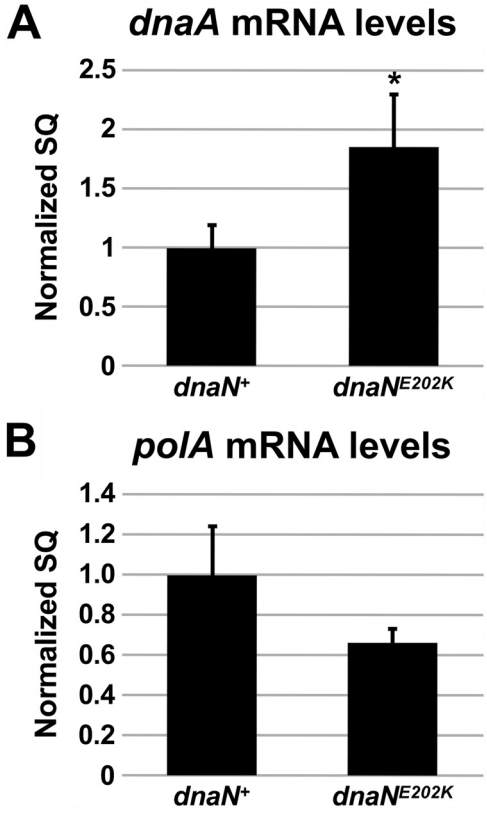

FIG 3 Altered *dnaA* and *polA* transcript levels in the *dnaN*^{E202K} mutant. Relative levels of the *dnaA* (A) and *polA* transcripts (B) in the *dnaN*$^{+}$ and *dnaN*^{E202K} strains were measured by qPCR. Results represent the average of 3 independent determinations ± SD. *, $P \leq 0.05$ (Student's *t* test) relative to the *dnaN*$^{+}$ control.

were compared with *nrdB* transcripts of the wild-type parent strain, which were normalized to one. Western blots that quantified the relative amounts of NrdB confirmed the relative decrease associated with the Δ*hda* mutation (Fig. 4B and C, lane 3 versus 5). Comparing the Δ*diaA dnaN*$^{+}$ strain with the wild-type control, the increased *nrdB* transcripts and NrdB protein levels confirm previous results (51).

For the Δ*hda* strain suppressed by plasmid pRM100, compared with the *hda*$^{+}$ strain bearing this plasmid, we observed both reduced *nrdB* transcript levels (Fig. 4A) and NrdB protein levels (Fig. 4B and C), consistent with published results (51).

Concurrently, we performed similar analyses, but with the isogenic strains carrying the *dnaN*^{E202K} allele instead of *dnaN*$^{+}$. Compared with the Δ*diaA* strain, the absence of *hda* resulted in significantly reduced levels of the *nrdB* transcript (Fig. 4A) and NrdB protein (Fig. 4B and C). Similar results were observed in comparing the *hda*$^{+}$ strain bearing pRM100 with its isogenic counterpart also carrying the plasmid but lacking *hda* (Fig. 4A to C). Taken together, these results indicate that *hda* function is required for the elevated *nrdAB* expression observed in the *dnaN*^{E202K} strain.

As added support, we used an established bacterial plating assay that measures the toxicity caused by hydroxyurea (HU) (51). HU inhibits NrdAB function by quenching the tyrosyl radical in NrdB (53, 54), but toxicity has been suggested to result primarily from DNA damage induced by one or more breakdown products of HU (55). However, we recently showed that the HU-resistant phenotype of the *dnaN*^{E202K} mutant is not the result of an enhanced activity in DNA repair or tolerance to DNA damage (25). Rather, plasmids that express elevated cellular levels of NrdB (51) or Hda protein (Fig. 5D) confer increased HU resistance. In contrast, the absence of *hda* that reduces the cellular level of NrdAB leads to severe HU sensitivity (Fig. 4) (51). As summarized in Fig. 4D, either the lack of *diaA* or the

Downloaded from https://journals.asm.org/journal/jb on 24 January 2022 by 35.10.240.139.

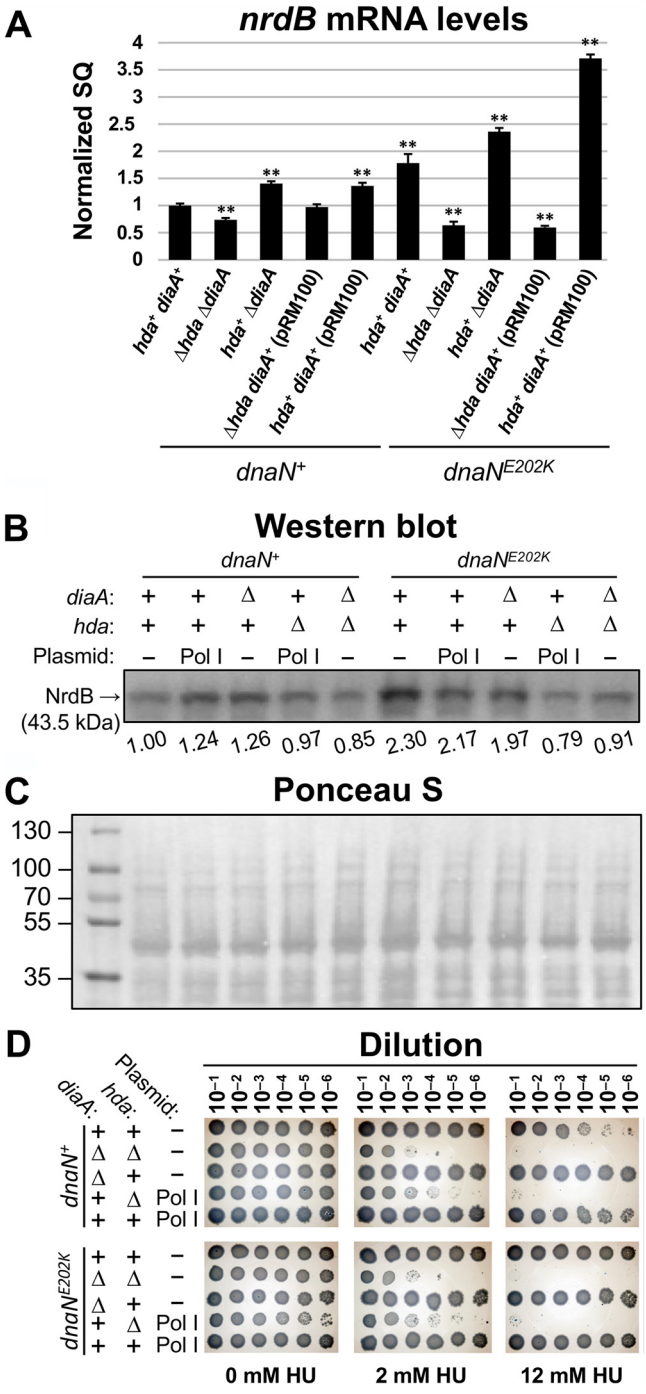

FIG 4 *hda* is required for elevated *nrdAB* expression in the *dnaN*^{E202K} mutant. (A) Respective levels of *nrdB* transcript in the indicated strains were measured by qPCR. The values shown represent the average of 3 independent determinations ± SD relative to the *dnaN*$^{+}$ *diaA*$^{+}$ *hda*$^{+}$ control that was set to 1. **, $P \leq 0.001$ (Student's *t* test) relative to the *dnaN*$^{+}$ *diaA*$^{+}$ *hda*$^{+}$ control. (B) Relative levels of NrdB protein in each strain were measured by Western blotting. Values represent the average of two independent experiments and are expressed relative to the wild-type control that was set equal to 1. (C) Equal transfer to the PVDF membrane in panel B was confirmed by staining with Ponceau S prior to Western blot analysis. (D) HU sensitivity was measured for isogenic *dnaN*$^{+}$ and *dnaN*^{E202K} strains that also bear other mutations and/or pRM100, a low-copy-number plasmid carrying *polA*, and the N-terminal coding region of *yihG* (*yihG'*). Results shown are representative of 3 independent experiments.

Downloaded from https://journals.asm.org/journal/jb on 24 January 2022 by 35.10.240.139.

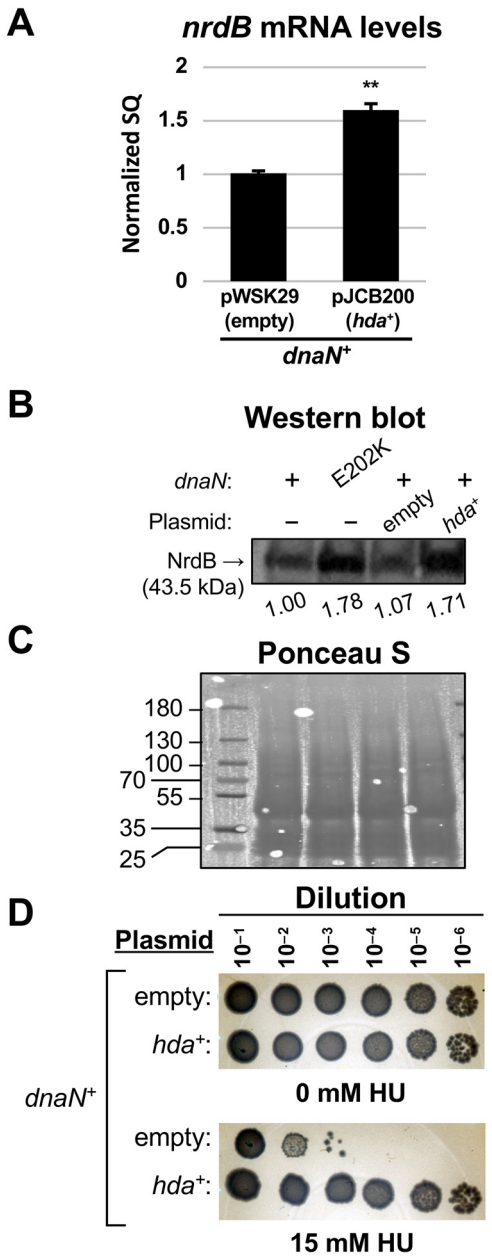

FIG 5 The Hda-overexpressing strain phenocopies the *dnaN*^{E202K} mutant (A and B). *nrdB* transcript levels (A) and NrdB protein levels (B) were measured for strain MG1655, this strain bearing the empty plasmid control (pWSK29), or the Hda-expressing plasmid (pJBC200) as indicated. Results represent the average of 3 determinations ± SD for qPCR or 2 determinations for the Western blot analysis. NrdB protein levels in panel B are relative to MG1655 lacking a plasmid, which was set equal to 1. **, $P \leq 0.001$ (Student's *t* test) relative to the pWSK29 control. (C) The PVDF membrane in panel B was stained with Ponceau S prior to Western blot analysis to confirm equal transfer of proteins. (D) HU sensitivity was measured for MG1655 bearing the empty plasmid control (pWSK29) or the Hda-expressing plasmid (pJBC200).

presence of plasmid pRM100 also conferred HU resistance compared with the wild-type control, in keeping with an elevated cellular level of NrdAB in these strains. Confirming published results (22, 51), *dnaN*^{E202K} or *dnaN*$^{+}$ strains expressing an elevated level of NrdB were HU resistant (Fig. 4D). The latter observations are further evidence that *hda* function is required for the elevated *nrdAB* expression in the *dnaN*^{E202K} strain. As a control, we measured the doubling times for each of these strains. Consistent with previous results demonstrating that the Δ*diaA* allele and the Pol I-expressing plasmid pRM100 efficiently

Downloaded from https://journals.asm.org/journal/jb on 24 January 2022 by 35.10.240.139.

TABLE 2 Doubling times for isogenic *E. coli* strains bearing suppressors of the Δ*hda* growth defect

	Relevant genotype[c]				
Strain[a]	*dnaN*	*diaA*	pRM100 (Pol I)	*hda*	Doubling time (min)[b]
VB001	+	+	−	+	41.1 ± 2.6
VB002	+	Δ	−	+	41.1 ± 2.6
VB003	+	Δ	−	Δ	41.2 ± 1.6
VB001 (pRM100)	+	+	+	+	42.5 ± 3.3
VB004	+	+	+	Δ	42.9 ± 2.6
VB019	E202K	+	−	+	43.1 ± 1.8
VB020	E202K	Δ	−	+	44.3 ± 2.8*
VB021	E202K	Δ	−	Δ	43.3 ± 3.3
VB019 (pRM100)	E202K	+	+	+	44.7 ± 3.9
VB022	E202K	+	+	Δ	47.0 ± 2.7**

[a]Strains are described in Table 5.
[b]Doubling time represents the average of 8 replicates ± SD. Cultures were grown in a sterile microtiter plate, so doubling times are slightly longer than they would be than if grown in tubes with more efficient aeration. *, $P \leq 0.05$; **, $P \leq 0.001$ (Student's *t* test) relative to the wild-type VB001 control.
[c]Symbols: +, wild-type gene or pRM100 is present; Δ, gene has been deleted; −, pRM100 is absent.

suppressed the growth defect of the *dnaN*$^+$ Δ*hda* strain (51), the doubling time for each strain was comparable with the VB001 wild-type control (Table 2). For *E. coli* VB020 that carries the *dnaN*^{E202K} mutation instead of the wild-type gene (relevant genotype, *dnaN*^{E202K} Δ*diaA hda*$^+$), the doubling time was ~3 min slower than the wild-type control (44.3 min versus 41.1), while the doubling time for VB022 (relevant genotype, *dnaN*^{E202K} *diaA*$^+$ Δ*hda* pRM100) was ~6 min slower (47.0 versus 41.1 min). Thus, the Δ*diaA* Pol I-expressing plasmid does not appear to fully suppress the growth defect conferred by Δ*hda* in the *dnaN*^{E202K} background.

The β^{E202K} clamp and the wild-type clamp interact similarly with Hda to stimulate the ATPase activity of DnaA. Results of the genetic assays presented above suggest that β^{E202K} is more active than the wild-type clamp in the hydrolysis of ATP bound to DnaA. As a test of this hypothesis, we used an established two-stage *in vitro* assay that measures DnaA activity in *oriC*-dependent DNA replication (56). In the first stage, Hda complexed with the β clamp and DnaA catalyzes the conversion of DnaA-ATP to DnaA-ADP. This leads to a reduction in the DnaA-ATP/DnaA-ADP ratio, which, in the second stage, reduces the level of DnaA-ATP-dependent *oriC* replication. In comparison with wild-type β, a low level of the β^{E202K} mutant (4.5 ng or 2.3 nM) was largely inactive (Fig. 6A). However, we recently demonstrated that this level of the β^{E202K} clamp was insufficient for supporting wild-type levels of Pol III replication in an *in vitro oriC*-dependent replication assay (25). When assayed at a higher level (56 ng or 28 nM), β^{E202K} was comparable with the wild-type β clamp (Fig. 6A, inset). Direct measurement of the hydrolysis of ATP bound to DnaA, which was dependent on Hda, demonstrated that the mutant was similar with the wild-type β clamp (Fig. 6B). We conclude that β^{E202K} is able to support the Hda-dependent hydrolysis of ATP bound to DnaA *in vitro*, and we suggest that its marginal activity at lower clamp levels (4.5 ng or 2.3 nM) (Fig. 6A) is a result of its increased affinity for the Pol IIIα catalytic subunit and apparent reduced affinity for the Pol III$\varepsilon\theta$ proofreading subunit, which impedes Pol III replication (25) that is required for the second stage of the *in vitro* assay.

As our *in vitro* assay is an indirect measure of the ability of the β clamp to interact with Hda, the results do not necessarily indicate that the E202K substitution has no effect on the affinity of the β clamp for Hda. To determine if β^{E202K} may form a more stable complex with Hda than the wild-type clamp, which may explain its apparently enhanced ability to support Hda activity *in vivo*, we performed surface plasmon resonance (SPR) and biolayer interferometry (BLI) experiments to quantify their binding. On the basis of the X-ray crystal structure of the Hda-β clamp complex, two discrete surfaces of Hda contact separate sites on the clamp (Fig. 1B) (57). Consistent with the X-ray structure, kinetic analysis of the SPR sensorgrams fit well to a two-site model. As summarized in Table 3,

Downloaded from https://journals.asm.org/journal/jb on 24 January 2022 by 35.10.240.139.

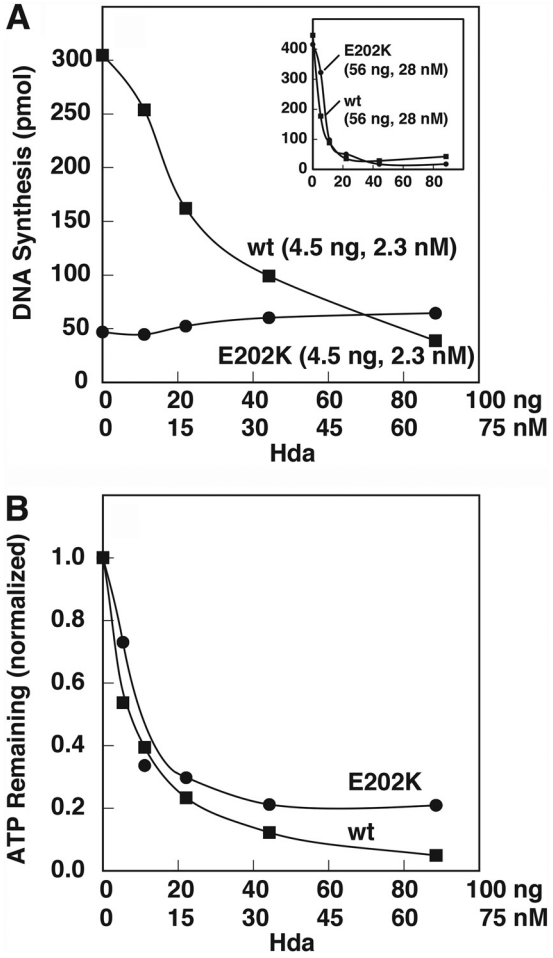

FIG 6 The β^{E202K} clamp supports Hda function in regulatory inactivation of DnaA (RIDA) *in vitro*. Assays comparing the *in vitro* activity of the wild-type β clamp with the β^{E202K} clamp in Hda- and β clamp-dependent RIDA at low and high levels (inset) of the β clamp (A) and the intrinsic DNA-dependent ATPase activity of DnaA (B). The *y* axis in panel B reflects the amount of ATP versus (ATP + ADP).

both clamp proteins displayed similar affinities for Hda *in vitro*, with equilibrium dissociation constant (K_D) values of 6.38 ± 1.82 nM (K_{D1}) and 36.2 ± 0.20 nM (K_{D2}) for the wild-type β clamp and 8.44 ± 0.35 nM (K_{D1}) and 50.5 ± 6.30 nM (K_{D2}) for β^{E202K}. The on rates (k_a) and off rates (k_d) were also similar. In addition to the β clamp, Hda requires an ADP cofactor to stimulate ATP hydrolysis by DnaA-ATP *in vitro* (11, 58). Binding of ADP serves to stabilize the active form of Hda (58). We therefore measured clamp-Hda interactions in the presence of ADP using BLI. As summarized in Table 4, both clamp proteins displayed similar affinities for Hda under these conditions. Moreover, the steady-state level of β^{E202K} is comparable with that of the wild-type clamp in exponentially growing cells (25), which excludes an explanation that the greater abundance of the mutant clamp is responsible for its behavior *in vivo*. However, the β^{E202K}-Hda complex may remain bound to DNA for a longer period. We plan to address this possibility in future work. Taken together, these findings indicate that the β^{E202K} clamp does not form a more stable complex with Hda.

Elevated levels of RNR suppress the toxicity caused by elevated levels of the β clamp. Elevated levels of RNR can enhance the efficiency of replication by increasing the supply of dNTPs (59). In light of this, we hypothesized that the increased level of the *nrdAB*-encoded RNR expressed in the *dnaN*^{E202K} strain (Fig. 4) served to suppress the toxicity caused by the elevated cellular abundance of the β clamp. To test this hypothesis, we used a wild-type strain (MG1655) bearing plasmids encoding *dnaN*$^{+}$

Downloaded from https://journals.asm.org/journal/jb on 24 January 2022 by 35.10.240.139.

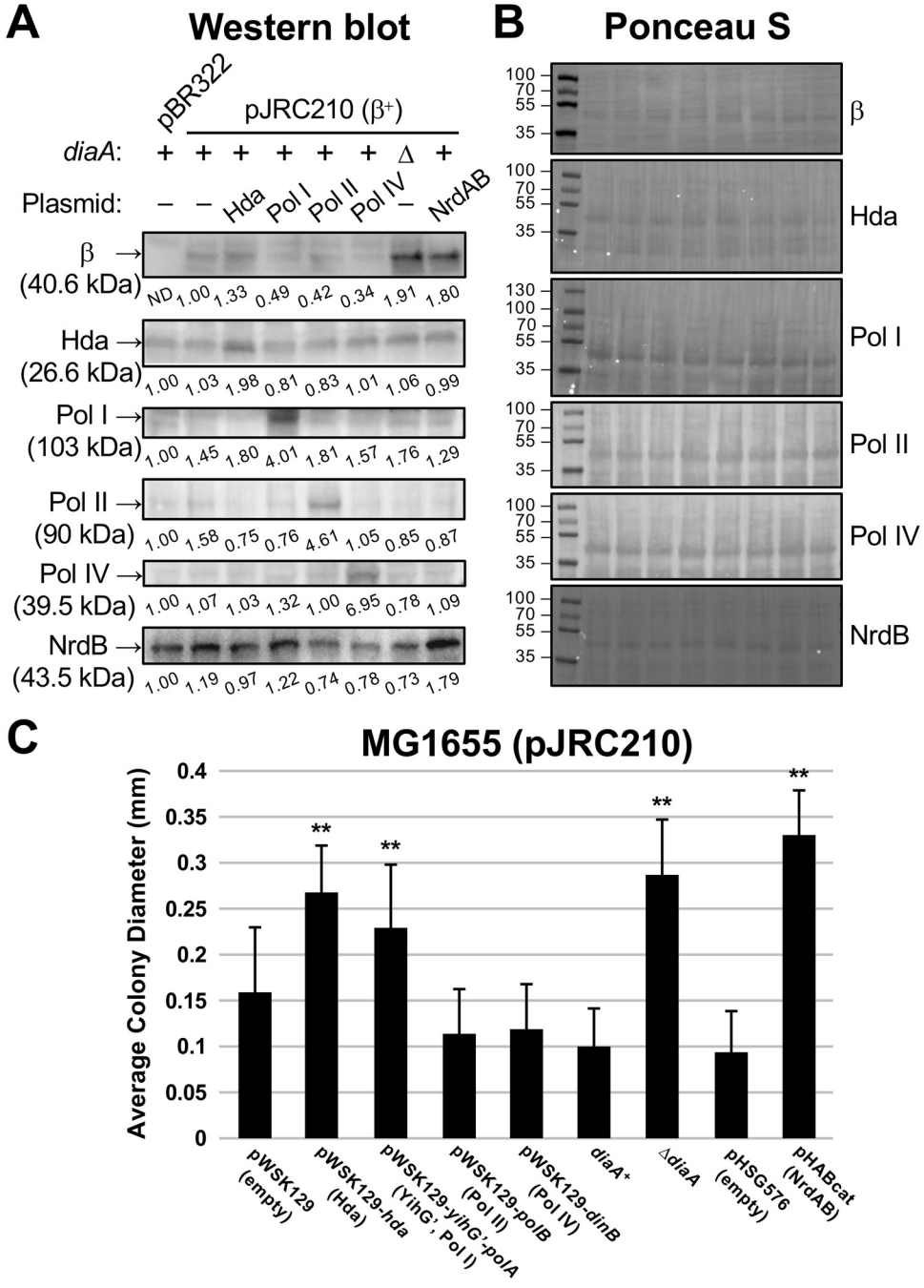

FIG 7 Increased cellular levels of the NrdAB proteins alleviate the toxic effect of elevated levels of the β clamp. (A) Western blot analysis was performed to measure the levels of the β clamp, Hda, Pol I, Pol II, Pol IV, and NrdB in various MG1655 strains. The values shown are relative to the control and representative of the average of two independent experiments. (B) Equal transfer to the PVDF membrane was confirmed for each membrane by its staining with Ponceau S prior to Western blot analysis. (C) Bar graph representation of the average diameter of 20 randomly selected colonies for each indicated strain following 18 h of growth at 30°C on LB $\pm$ SD. **, $P \leq 0.001$ (Dunnett's multiple-comparison test) relative to the MG1655 control lacking a plasmid (see the bar in panel C labeled *diaA*$^+$).

(pJRC210), *dnaN*^{E202K} (pJRCHA7.1), or pBR322 as a control. Using these plasmid-bearing strains, we previously demonstrated that both the wild-type clamp and the β^{E202K} mutant were expressed at a level that was ~10-fold higher than the empty control plasmid (22). We confirmed elevated expression of the β clamp compared with the control strain bearing pBR322 (Fig. 7A and B), but the endogenously expressed clamp was not

Downloaded from https://journals.asm.org/journal/jb on 24 January 2022 by 35.10.240.139.

TABLE 3 Interaction of Hda with the wild-type β and β^{E202K} clamp proteins

Interaction[a]	Expt	K_D (nM)	k_a ($M^{-1}s^{-1}$)	K_d (s^{-1})	Avg (range)[b] K_{D1}	Avg (range)[b] K_{D2}
$^{His}\beta$-Hda	1	K_{D1}, 5.47	2.23×10^4	1.22×10^{-4}	6.38 (1.82)	36.2 (0.20)
		K_{D2}, 36.1	1.66×10^5	6.01×10^{-3}		
	2	K_{D1}, 7.29	2.13×10^4	1.56×10^{-4}		
		K_{D2}, 36.3	1.71×10^5	6.21×10^{-3}		
$^{His}\beta^{E202K}$-Hda	1	K_{D1}, 8.26	2.00×10^4	1.65×10^{-4}	8.44 (0.35)	50.5 (6.30)
		K_{D2}, 53.6	1.25×10^5	6.72×10^{-3}		
	2	K_{D1}, 8.61	1.80×10^4	1.55×10^{-4}		
		K_{D2}, 47.3	1.28×10^5	6.08×10^{-3}		

[a]The indicated His_6-tagged clamp protein (ligand) was attached to the SPR sensor surface using penta-His antibody (Qiagen), while the untagged Hda protein (analyte) was flowed over the sensor surface. Interactions were analyzed using the two-site binding model. Instead of χ^2 (goodness of fit), the ClampXP 3.50 software provides residual sum-of-squares (goodness of fit), which were each <10% of the respective R_{max}, confirming the specificity of each interaction.

[b]Average of 2 independent experiments, each examining 5 different concentrations (60 to 960 nM) of analyte (Hda) ± range.

detected (Fig. 7A). Plating experiments revealed that the strain with an elevated level of the wild-type β clamp compared with the control exhibited a severe growth defect at 30°C, as measured by colony size. This is in contrast with the benign effects of the β^{E202K} clamp or pBR322 control under comparable conditions (Fig. 7C). Where indicated, we transformed these strains with a second compatible plasmid (pHABcat) that expresses NrdAB at ~2-fold higher levels than the control strain (Fig. 7A and B). The strain with both an elevated level of the β clamp and the *nrdAB*-expressing plasmid (pHABcat), but not the empty plasmid (pHSG576), failed to display a growth defect (Fig. 7C). These observations support our hypothesis that an increased level of NrdAB suppresses the toxicity caused by the elevated abundance of the β clamp. We consider additional mechanisms in the Discussion.

Despite elevated NrdAB levels, the *dnaN*^{E202K} mutant displays a near-wild-type spontaneous mutation frequency. Others have described that elevated RNR or cellular dNTP levels suppress proofreading by Pol IIIε (60). Thus, we hypothesized that the *dnaN*^{E202K} strain would exhibit an elevated spontaneous mutation frequency compared with the *dnaN*$^+$ control due to an increased abundance of RNR and dNTPs. However, the incidence of spontaneous rifampin resistance (Rif^r) with the *dnaN*^{E202K} mutant (4.24×10^{-8}) and the *dnaN*$^+$ strain (3.33×10^{-8}) was statistically indistinguishable (Fig. 8A). As a control, we transformed the wild-type strain with a plasmid that expresses *E. coli* NrdAB at ~2.7-fold higher than chromosomally expressed levels (Fig. 8C and D). The median frequency of spontaneous Rif^r of the

TABLE 4 Interaction of Hda with the wild-type β and β^{E202K} clamp proteins in the presence of ADP

Interaction[a]	Expt	K_D (nM)	k_a ($M^{-1}s^{-1}$)	K_d (s^{-1})	Avg (range)[b] K_{D1}	Avg (range)[b] K_{D2}
$^{His}\beta$-Hda	1	K_{D1}, 5.70	1.30×10^5	7.50×10^{-4}	5.05 (1.30)	66.0 (3.90)
		K_{D2}, 67.9	3.50×10^5	2.38×10^{-2}		
	2	K_{D1}, 4.40	1.32×10^5	5.80×10^{-4}		
		K_{D2}, 64.0	3.28×10^5	2.10×10^{-2}		
$^{His}\beta^{E202K}$-Hda	1	K_{D1}, 6.29	1.36×10^5	8.57×10^{-4}	5.24 (2.10)	51.8 (1.00)
		K_{D2}, 52.3	4.67×10^5	2.44×10^{-2}		
	2	K_{D1}, 4.19	1.32×10^5	5.53×10^{-4}		
		K_{D2}, 51.3	3.56×10^5	1.82×10^{-2}		

[a]The indicated His_6-tagged clamp protein (ligand) was captured using the BLI Penta-His (HIS1K) Dip and Read biosensor tips, and interactions with untagged analyte were measured in HSB-EP supplemented with magnesium acetate and ADP using an Octet Red 96e BLI instrument (Sartorius). χ^2 values (likelihood of no relationship) ranged from 0.0644 to 0.0823, while R^2 (goodness of fit) ranged from 0.9994 to 0.9996 for each fit to the 2:1 heterogenous ligand model.

[b]Average of 2 independent experiments, each examining 4 different concentrations (50 to 140 nM) of analyte (Hda) ± range.

Downloaded from https://journals.asm.org/journal/jb on 24 January 2022 by 35.10.240.139.

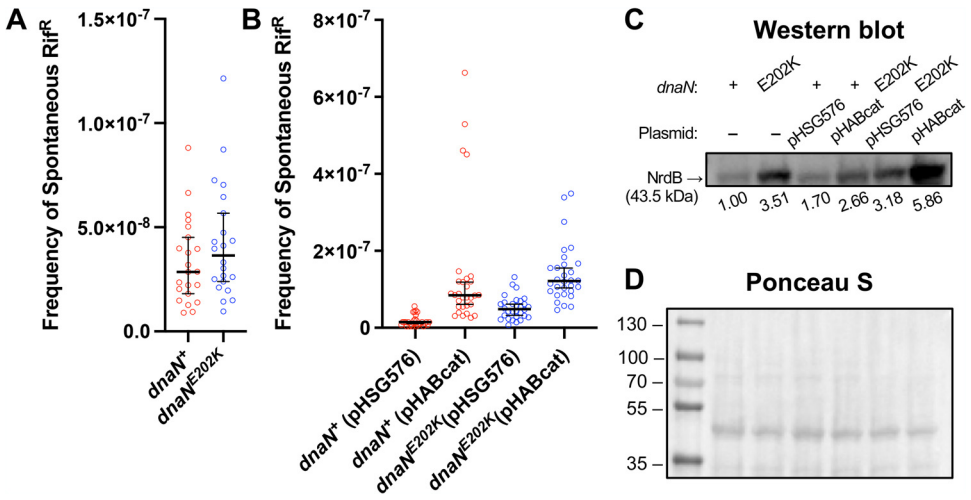

FIG 8 The *dnaN*^{E202K} strain fails to exhibit an elevated frequency of spontaneous Rif^r despite its elevated NrdAB levels. The frequency of spontaneous Rif^r was measured for the *dnaN*$^+$ and *dnaN*^{E202K} strains either lacking a plasmid (n = 22 for each strain) (A) or these same strains bearing plasmid pHSG576 (empty control) or pHABcat (*nrdAB*) (B), as indicated (n = 30 for each strain). Each open circle represents a single measured frequency of spontaneous Rif^r. The bar represents the median frequency of spontaneous Rif^r, while the error bars represent 95% confidence intervals. Panels A and B were generated using GraphPad Prism. (C) NrdB levels were measured by Western blotting. The values shown are relative to the wild-type control and represent the average of two determinations. (D) Equal transfer to the PVDF membrane was confirmed by its staining with Ponceau S prior to Western blot analysis.

dnaN$^+$ NrdAB-overexpressing strain was almost 6-fold higher than the same strain bearing the empty control plasmid (Fig. 8B) (8.45×10^{-8} versus 1.49×10^{-8}). Likewise, an increased frequency of spontaneous Rif^r was observed with the *dnaN*^{E202K} mutant bearing the *nrdAB*-expressing plasmid (1.21×10^{-7}). However, this strain expressed more than twice the level of NrdAB than the wild-type strain bearing the same plasmid (Fig. 8C and D). Taken together, these results suggest that β^{E202K} somehow renders Pol III able to maintain its ability to accurately synthesize DNA when cellular dNTP levels are elevated.

DISCUSSION

In recent work, we found that an ~10-fold increased abundance of the wild-type clamp impedes *E. coli* growth (22). Based on the properties of other mutant clamps, which are defective in binding to Pol III, we proposed a model that attributes the toxicity caused by an elevated cellular abundance of the β clamp to sequestration of Pol III so that it is unable to synthesize DNA (25). Results from that study also indicate that the β^{E202K} mutant clamp is not deficient in its interaction with Pol III but, instead, has a higher affinity for the DNA polymerase than the wild-type clamp. Hence, an alternate mechanism explains its inability to impede *E. coli* growth when expressed at an elevated cellular level (25). Herein, we describe that an ~2-fold increase in the abundance of RNR via a plasmid suppresses the toxic effect of an ~10-fold increase of the β clamp (Fig. 7). Thus, β^{E202K} at an otherwise toxic level permits growth because the *dnaN*^{E202K} strain expresses RNR at a higher and neutralizing level compared with a *dnaN*$^+$ strain (Fig. 4 and 7). Taken together, these results suggest that the relative levels of the β clamp and NrdAB are critical for *E. coli* viability. This regulatory pathway is directly connected with transcriptional regulation of the *nrdAB* and *dnaAN* operons (40, 61, 62), and by the DnaA-ATP/DnaA-ADP ratio (40), which, in turn, is regulated in large part by the β clamp-Hda complex (11, 61).

In light of the suppressive effect of RNR described above, other conditions that lead to increased NrdAB levels should similarly suppress. Our experiments to test this idea yielded mixed results. We previously reported substantially enhanced *nrdAB* transcription in strains lacking *diaA* (51). Confirming the expectation of suppression, the Δ*diaA*

Downloaded from https://journals.asm.org/journal/jb on 24 January 2022 by 35.10.240.139.

mutation offset the growth defect conferred by a plasmid that increased the abundance of the β clamp by ~10-fold (Fig. 7), but, surprisingly, the Δ*diaA* strain expressing an elevated level of the β clamp did not show increased NrdB levels (Fig. 7A and B). Plasmids carrying either Hda or the *polA-yihG′* region similarly restored normal growth to a strain that should have an elevated abundance of the β clamp (Fig. 7C). However, although the strain bearing the Hda plasmid correlated with an increase of NrdB (Fig. 5) (51), this strain carrying an additional plasmid expressing the β clamp did not have an increased NrdAB level (Fig. 7A). In contrast, the plasmid carrying the *polA-yihG′* region led to increased expression of NrdB by 1.2-fold (Fig. 7A) but reduced the level of the β clamp by ~2-fold. As controls for the Pol I-expressing plasmid, plasmids expressing elevated levels of Pol II (pRM101; ~4.5-fold elevated level) or Pol IV (pRM102; ~7-fold elevated level) failed to influence NrdB levels (Fig. 7A and B) and did not suppress the growth defect caused by an elevated level of the β clamp (Fig. 7C). However, these plasmids encoding Pol II or Pol IV led to 2.5- to 3-fold lower β clamp levels than the strain carrying the wild-type clamp-expressing plasmid alone (Fig. 7A and B). With the exception of the plasmid expressing elevated levels of NrdAB (pHABcat), the results do not correlate suppression of the growth defect caused by elevated cellular levels of the β clamp with elevated NrdB levels (Fig. 7). Considering this finding and also the large number of clamp partners, the β^{E202K} mutant may exhibit multiple effects in parallel, one or more of which may add to the suppression of the growth defect. For example, in addition to the elevated NrdAB levels, the underinitiation phenotype of the *dnaN*^{E202K} mutant (Fig. 2) may also contribute to the suppression of the growth defect caused by elevated levels of the β clamp. Specifically, hypoinitiation should reduce the probability of a replication fork colliding with one arising from the prior replication cycle that is stalled, presumably leading to fewer lethal double-strand breaks. Thus, several independent mechanisms conferred by *dnaN*^{E202K} may contribute to suppression. Likewise, distinct molecular mechanisms may explain the basis for suppression by other *dnaN* mutants.

The behavior of the *dnaN*^{E202K} strain supports the expectation that β^{E202K} may be more active than the wild-type clamp in stimulating the hydrolysis of ATP bound to DnaA. Specifically, the *dnaN*^{E202K} mutant (i) underinitiates DNA replication apparently from a lower DnaA-ATP/DnaA-ADP ratio (Fig. 2), (ii) displays altered expression of several DnaA-regulated genes (Fig. 3 and Table 1), (iii) relies on *hda* function for increased *nrdAB* transcription (Fig. 4), and (iv) phenocopies the *dnaN*$^{+}$ strain expressing an elevated cellular level of Hda (Fig. 5). However, β^{E202K} or the wild-type clamp stimulated ATP hydrolysis similarly when assayed at higher levels and combined with Hda (Fig. 6), indicating that β^{E202K} is not more active than its wild-type counterpart. We discuss several models for the apparent discrepancy between the *in vivo* and *in vitro* results. It is important to keep in mind that these models are neither exclusive nor independent of each other, and more than one may contribute to the observed phenotypes. As such, one or more may explain the apparent discrepancy.

The loading of the β clamp onto DNA involves its direct interaction with the δ subunit of the DnaX clamp loader complex, followed by its interaction with Pol III to stabilize the replicase at a primer terminus (20, 63). In the first model, the mutant clamp has a higher affinity for the δ subunit, leading to more β^{E202K} clamps on DNA able to form complexes with Hda followed by a lower DnaA-ATP/DnaA-ADP ratio. However, we showed that the wild-type clamp and β^{E202K} have similar affinities for the δ subunit of the DnaX complex (25), as well as for Hda-ADP (Table 4). Thus, it is unlikely that the *dnaN*^{E202K} strain supports a higher level of β^{E202K}-Hda complexes *in vivo* than the wild-type strain.

A second model hypothesizes that β^{E202K} has a lesser affinity for other clamp partners but retains its affinity for Hda and the δ subunit of the DnaX complex. As a result, more β^{E202K}-Hda complexes form in a *dnaN*^{E202K} mutant than a wild-type strain. That our *in vitro* assay lacks other clamp partners may explain the comparable activities of the wild-type and β^{E202K} clamp proteins. We attempted to address if β^{E202K} has a

Downloaded from https://journals.asm.org/journal/jb on 24 January 2022 by 35.10.240.139.

weaker affinity for Pol I, Pol V, DNA ligase, MutS, MtL, and/or CrfC. In one series of experiments, we failed to observe any significant effects of the interaction of β^{E202K} with Pol II and Pol IV (25). We also were unable to reliably measure interactions of the clamp with Pol I or Pol V by BLI *in vitro*. However, the *dnaN*^{E202K} strain supports normal levels of Pol V mutagenesis (25), suggesting that β^{E202K} interacts normally with the *umuDC* gene products. The *dnaN*^{E202K} strain also fails to display an elevated frequency of spontaneous Rif^r (Fig. 8A); even though Rif^r is not the most sensitive measure of a mismatch repair deficiency, as it does not measure frameshift mutations (64), these findings nevertheless suggest that the β^{E202K} clamp interacts normally with MutSL. In other work, we were unable to measure the levels of Hda and DnaA on DNA using chromatin immunoprecipitation due to the lack of specificity of our antibody preparations (unpublished results). Despite the evidence being incomplete, the β clamp appears to have a much higher affinity for Hda than most, if not all, other partners (65). Thus, this model is unlikely to explain the apparent discrepancy between our *in vivo* and *in vitro* results.

A third model is based on our finding that β^{E202K} possesses a higher affinity for Pol III core compared with wild-type β (25), suggesting that the β^{E202K}-Hda complex stimulates the hydrolysis of ATP bound to DnaA as Pol III copies DNA. Consistent with this possibility, studies suggest that an actively replicating Pol III stimulates ATP hydrolysis by DnaA (66–68). If so, the inability to observe higher activity *in vitro* by the β^{E202K} clamp than the wild-type clamp may be attributed to a limited window of opportunity; for a 7-kb duplex DNA molecule duplicated bidirectionally from *oriC* at an *in vitro* rate of ~400 nucleotides per second, the 9 s required for its complete replication may be insufficient to detect a difference. While this model is formally possible, it nevertheless seems unlikely that a longer lasting interaction of Hda with the mutant clamp as part of the Pol III HE complex would necessarily lead to enhanced Hda activity.

A fourth model is based on the suggestion that the *Bacillus subtilis* YabA protein simultaneously binds both the β clamp and DnaA-ATP to sequester DnaA-ATP away from *oriC* (69). It is possible that the *E. coli* β^{E202K}-Hda complex acts similarly to effectively reduce the DnaA-ATP/DnaA-ADP ratio. The crystal structure of the β clamp-Hda complex suggests that it must undergo significant structural rearrangement to support ATP hydrolysis by DnaA (57). Although we failed to observe a significant effect of the E202K mutation on the interaction of the clamp with Hda *in vitro*, given the location of E202 relative to the known Hda binding surfaces (Fig. 1B), β^{E202K} may better adopt a conformation over the wild-type clamp in the β^{E202K}-Hda complex for the sequestration of DnaA-ATP. While further work is required to determine whether the β^{E202K}-Hda complex sequesters DnaA-ATP, a noncatalytic role for Hda could explain the apparent discrepancy between the *in vivo* and *in vitro* results regarding the ability of the β^{E202K}-Hda complex to reduce the cellular DnaA-ATP/DnaA-ADP ratio. Alternatively, a combination of the models discussed may be responsible.

We also determined that the *dnaN*^{E202K} mutant, compared with the isogenic *dnaN*$^+$ strain, expresses a higher level of *nrdAB* but is less sensitive to the increased abundance of RNR. Pol III favors nucleotide incorporation over proofreading when dNTP levels are elevated (59, 60). As a result, strains expressing elevated cellular levels of NrdAB display an increased spontaneous mutation frequency compared with a control strain with the normal NrdAB level due to lower Pol III proofreading activity (60). We recently determined that the E202K mutation changes the way in which the clamp interacts with the Pol III$\alpha\varepsilon\theta$ core complex (25). This alteration likely explains why Pol III in the *dnaN*^{E202K} strain does not have an elevated frequency of spontaneous Rif^r (Fig. 8A). We suggest that the β clamp interacts dynamically with Pol IIIα and Pol IIIε and that the E202K mutation affects these dynamics to alter how the clamp manages the polymerase and exonuclease proofreading activities to maintain the fidelity of DNA replication by Pol III. An alternate model considers that Pol II proofreads Pol III errors (70). Thus, the E202K mutation may influence the exchange of Pol III and Pol II on the β clamp to reduce the frequency of spontaneous mutation. However, our finding that the wild-

Downloaded from https://journals.asm.org/journal/jb on 24 January 2022 by 35.10.240.139.

TABLE 5 *E. coli* strains and plasmids

Strain or plasmid	Relevant genotype or characteristics	Source or reference
E. coli strains		
BL21(DE3)	*ompT gal dcm lon hsdSB* (r_B- r_B-) λ(DE3 [*lacI lacUV5-T7p07 ind1 sam7 nin5*])	Novagen
MG1655	*ilvG* mutant *rfb-50 rph-1*	*E. coli* Genetic Stock Center
VB001	MG1655 *dnaN*$^+$-*tet*$^+$-*recF*$^+$	51
VB019	MG1655 *dnaN*^{E202K}-*tet*$^+$-*recF*$^+$	25
VB002	MG1655 *dnaN*$^+$-*tet*$^+$-*recF*$^+$ Δ*diaA762*::*kan*	51
VB020	MG1655 *dnaN*^{E202K}-*tet*$^+$-*recF*$^+$ Δ*diaA762*::*kan*	This work
VB003	MG1655 *dnaN*$^+$-*tet*$^+$-*recF*$^+$ Δ*hda*::*cat* Δ*diaA762*::*kan*	51
VB021	MG1655 *dnaN*^{E202K}-*tet*$^+$-*recF*$^+$ Δ*hda*::*cat* Δ*diaA762*::*kan*	This work
VB004	MG1655 *dnaN*$^+$-*tet*$^+$-*recF*$^+$ Δ*hda*::*cat* (pRM100)	51
VB022	MG1655 *dnaN*^{E202K}-*tet*$^+$-*recF*$^+$ Δ*hda*::*cat* (pRM100)	This work
Plasmids		
pWSK29	Amp^r; pSC101 *oriV*; low-copy-no. cloning vector	78
pJCB200	Amp^r; pWSK29 derivative that expresses *hda*$^+$ from its native promoter	46
pRM100	Amp^r; pWSK29 derivative that bears the first 196 residues of *yihG*$^+$ and all of *polA*$^+$ (*yihG′-polA*$^+$), with each expressed from its native promoter	79
pWSK129	Kan^r; pSC101 *oriV*; low-copy-no. cloning vector	78
pWSK129-*hda*	Kan^r; pWSK129 derivative that expresses *hda*$^+$ from its native promoter	This work
pWSK129-*yigH′-polA*	Kan^r; pWSK129 derivative that bears the first 196 residues of *yihG*$^+$ and all of *polA*$^+$ (*yihG′-polA*$^+$), with each expressed from its native promoter	This work
pWSK129-*polB*	Kan^r; pWSK129 derivative that expresses *polB*$^+$ (Pol II) from its native promoter	This work
pWSK129-*dinB*	Kan^r; pWSK129 derivative that expresses *dinB*$^+$ (Pol IV) from its native promoter	This work
pHSG576	Cam^r; pSC101 *oriV*; low-copy-no. cloning vector	80
pHABcat	Cam^r; pHSG576 derivative that expresses *nrdA*$^+$*B*$^+$ and the downstream *yfaE*$^+$ gene from their native promoters	81
pBR322	Amp^r; ColE1 *oriV*; cloning vector	Laboratory stock
pDS596	Amp^r; pBR322 derivative that overexpresses *dnaA*$^+$ from the *araBAD* promoter	82
pJRC210	Amp^r; pBR322 derivative that overexpresses *dnaN*$^+$ from the *tac* promoter	23
pJRCHA7.1	Amp^r; pBR322 derivative that overexpresses *dnaN*^{E202K} from the *tac* promoter	23
pβ^{HMK}	Amp^r; pET16b derivative that overexpresses β clamp bearing N-terminal His_6 and HMK[a] tags	20
pβE202K^{HMK}	Amp^r; pET16b derivative that overexpresses the β^{E202K} clamp bearing N-terminal His_6 and HMK tags	25
pETM11	Kan^r; pBR322 *oriV*; T7 overexpressing vector encoding an N-terminal His_6 tag that is removable by TEV cleavage	EMBL collection
pETM11-Hda	Kan^r; pETM11 derivative that overexpresses *hda*$^+$ from the T7 promoter	This work

[a]HMK, heart muscle kinase.

type clamp and β^{E202K} exhibited similar affinities for Pol II is not consistent with this model.

MATERIALS AND METHODS

Bacteriological techniques. *E. coli* strains and plasmid DNAs are described in Table 5. *E. coli* was transformed with plasmid DNAs using the $CaCl_2$ method as described previously (3). Unless otherwise noted, strains were cultured in Luria-Bertani medium (LB; 10 g/liter tryptone, 5 g/liter yeast extract, and 10 g/liter NaCl). When appropriate, the following antibiotics were used at the indicated concentrations: ampicillin (Amp), 150 μg/ml; chloramphenicol (Cam), 20 μg/ml; kanamycin (Kan), 40 μg/ml; rifampin (Rif), 50 μg/ml; and tetracycline (Tet), 10 μg/ml for strains bearing plasmids or 2.5 μg/ml for strains bearing the chromosomal *tet* allele between *dnaN* and *recF*.

Measurement of *E. coli* strain growth rate (doubling time). Separate overnight cultures of the indicated *E. coli* strains grown at 37°C in LB were used to inoculate (1:200) fresh LB cultures (200 μl) grown with shaking in a sterile 96-well microtiter plate (Corning) at 37°C using a FLUOstar Omega microplate reader (Ingen Technologies). Growth was monitored by measuring the change in optical density at 600 nm (OD_{600}) every 383 s. The doubling time for each strain was calculated using the doubling time cell calculator (Doubling Time Computing; http://www.doubling-time.com/compute.php); values represent the average of eight determinations ± standard deviation (SD).

Whole-transcriptome analysis. Whole-transcriptome analysis was performed with three biological replicates for each strain by the UB Genomics and Bioinformatics Core as described (51). Briefly, RNA was purified from exponential-phase cultures of isogenic *dnaN*$^+$ and *dnaN*^{E202K} strains grown at 37°C using phenol-chloroform and was depleted of rRNA using the bacterial Ribo-Zero rRNA removal kit (Illumina) as per the manufacturer's recommendations. After validating the quality of the RNA samples using a Bioanalyzer, libraries were constructed and subjected to rapid 100-cycle single-read sequencing using

Downloaded from https://journals.asm.org/journal/jb on 24 January 2022 by 35.10.240.139.

an Illumina next-generation sequencer. Generation of fragments per kilobase per million (FPKMs) was performed using Cufflinks 2.1.1. Log_2 fold change in FPKMs of *dnaN*^{E202K} transcripts compared with wild type were clustered using the Cluster 3.0 program with uncentered correlation similarity metric via the average linkage clustering method. Select results for the wild-type and *dnaN*^{E202K} strains were published previously (25, 51).

Quantitative PCR. qPCR was performed with freshly prepared RNA samples distinct from those used in RNA-seq experiments using a Bio-Rad iCycler. Starting quantity (SQ) values were calculated from the threshold cycle (C_T) values after fitting to the standard curve obtained using genomic DNA standards as described (46). To control for variations between RNA samples, the SQ values were normalized to *hcaT* levels similarly determined by qPCR. Primers for qPCR were qNrdBFor (AATTATTCGCCTGATTGCCCGCGA), qNrdBRev (ACACTCTTCGGCAATTTCCGCCAT), qDnaAFor (TTGCCAATGCCAACTTTACCGGAC), qDnaARev (TGGAAAGGAGATCCGCGACTTTGA), qPolAFor (GCATCCTTTACCCATAATC), qPolARev (TTAGTGCGCCTGATCCCA), qhcaTFor (GCTCGGCTATTTCACATACT), and qhcaTRev (ATAACAGGCCGATGGTTTC).

Western blot analysis. Overnight cultures of the indicated strains were subcultured 1:100 in LB media to mid-exponential phase (OD_{600}, ~0.5). A volume equivalent to 2 ml of OD_{600} 0.5 culture was centrifuged, and each cell pellet was resuspended with 15 μl of B-PER protein extraction reagent (Pierce). Following addition of 35 μl of SDS loading dye (63 mM Tris-HCl [pH 6.8], 10% glycerol, 2% SDS, 0.005% bromophenol blue, and 10% 2-mercaptoethanol), the mixture was heated at 95°C for 10 min. Samples (10 μl) were separated by 12% SDS-PAGE and then transferred to polyvinylidene difluoride (PVDF) membranes using a Trans-Blot Turbo semidry transfer system (Bio-Rad). PVDF membranes were stained with Ponceau S prior to Western blot analysis to evaluate protein transfer. After destaining with 0.1 M NaOH, membranes were washed first with 1× TS (150 mM NaCl, 50 mM Tris-HCl [pH 7.6]) and then with 1× TS plus Tween (0.05%). Membranes were blocked with 1× TS-Tween (0.05%) plus 2% nonfat dry milk for 1 h prior to incubation with appropriate dilutions of the following rabbit antisera overnight at 4°C: anti-NrdB (1:10,000), anti-β clamp (1:50,000), anti-Hda (1:10,000), anti-Pol I (1:25,000), anti-Pol II (1:25,000), and anti-Pol IV (1:5,000). All antisera were produced using a University at Buffalo IACUC-approved protocol. After washing with TS-Tween, the membranes were probed with secondary goat anti-rabbit antibody (Bio-Rad) at a 1:25,000 dilution for 1 h, washed, and then treated with 1 ml of the Clarity Western ECL substrate mixture (Bio-Rad) for 2 min before visualizing with a ChemiDoc Imager (Bio-Rad).

Quantitation of HU sensitivity. HU was freshly prepared in sterile water at a concentration of 1 M and sterile filtering through a 0.22-μm filter (Millipore). HU sensitivity was measured by spotting 10-μl aliquots of 10-fold serial dilutions of the indicated overnight cultures onto agar plates containing the indicated concentration of HU. Plates were incubated overnight (16 h) before imaging.

Flow cytometry. Bacterial cells were cultured at 37°C with aeration for 4 h in M9 minimal medium supplemented with glucose and Casamino Acids. Genome content after replication runout was measured by flow cytometry and analyzed using a BD FACSCanto instrument and FlowJo 10.2 software as described previously (46, 51). The average cell mass was calculated as the average fluorescein isothiocyanate (FITC) (EMD Millipore) fluorescence. The average DNA/mass was calculated by dividing the average DNA content by the average cell mass.

DNAs and proteins. The supercoiled *oriC*-containing plasmid M13*oriC*2LB5 was purified as described (71, 72). Hda was purified from BL21(DE3) bearing pETM11-Hda, which expresses an N-terminally His_6-tagged form of the protein containing a tobacco etch virus (TEV) cleavage site between the His_6 tag and Hda. Cells were grown in LB media supplemented with Kan at 37°C to an OD_{600} of 0.4 to 0.6. The culture was moved to a 16°C shaking incubator, and protein overexpression was induced with 1 mM IPTG (isopropyl-β-D-thiogalactopyranoside) followed by incubation overnight at 16°C with shaking. Cells were pelleted and resuspended in buffer S [50 mM HEPES-KOH (pH 8.0), 50 mM NaCl, 10% glycerol, 1 mM Tris-(2-carboxyethyl)phosphine (TCEP), 0.01% Brij, 5 mM $Mg(CH_3COO)_2$ and 0.1 mM ADP] and lysed using a French press. The cell lysate was clarified by centrifugation at 10,000 × *g* for 15 min using a JA-17 rotor (Beckman Coulter). The supernatant was passed through a 0.2-μm polycarbonate filter (Millipore) before it was applied to a 5-ml HiTrap chelating column (GE Healthcare) charged with Ni^{2+} and preequilibrated in buffer S. Bound Hda was eluted with a linear gradient of 0 to 0.5 M imidazole in buffer S. The eluted sample was desalted using a 5-ml HiTrap desalting column (GE Healthcare) followed by cleavage of the His tag overnight on ice with acTEV protease (Invitrogen). The cleaved sample was passed through a 5-ml HiTrap chelating column charged with Ni^{+2} to purify untagged Hda that was collected in the flowthrough. Untagged and N-terminally His_6-tagged forms of the wild-type β and β^{E202K} clamps (24, 73), as well as other replication proteins (56, 74), were each purified as described. The concentration of each purified protein was determined by the dye binding method (75) and also by densitometric analysis of SDS-PAGE after staining with Coomassie blue using bovine serum albumin (BSA) to prepare a standard curve.

***In vitro* DNA replication of an *oriC*-containing plasmid.** Two-stage replication assays were performed as described previously with the indicated concentrations of Hda protein (56). Acid-insoluble radioactivity retained on glass fiber filters was measured by liquid scintillation spectrometry.

Hydrolysis of ATP bound to DnaA. Reactions to compare β^{E202K} with wild-type β for the hydrolysis of radiolabeled ATP bound to DnaA were assembled essentially as described (56). Briefly, DnaA (2 pmol) was incubated in reactions (2.5 μl) containing 1.5 μM [γ-^{32}P]ATP for 15 min at 0°C. A mixture containing wild-type β or β^{E202K} (56 ng), DNA polymerase III* (90 ng; 0.18 pmol), M13*oriC*2LB5 supercoiled DNA (200 ng; 46 fmol), and the indicated amounts of Hda was added to reactions (25 μl) containing 2 mM ATP and 30 μM ADP. After incubation for 20 min at 30°C, DnaA was immunoprecipitated with protein A-agarose beads that were preincubated with rabbit antiserum that specifically recognizes the DNA

Downloaded from https://journals.asm.org/journal/jb on 24 January 2022 by 35.10.240.139.

binding domain of DnaA. The relative amount of DnaA-bound nucleotide was quantified after polyethyleneimine-cellulose thin-layer chromatography.

Surface plasmon resonance. SPR experiments were conducted at 25°C using a kinetic titration approach with a dual-channel Reichert SR7500DC instrument as described (25, 76). Approximately 4,000 response units (RU) of the penta-His antibody (Qiagen) were bound on a 500-kDa carboxymethyl dextran chip (Reichert Inc.) by amine coupling to both channels as per the manufacturer's recommendation. Approximately 1,000 RU of β-His_6 or β^{E202K}-His_6 was captured in the left channel for 3 min at a flow rate of 25 μl/min, and 60 to 960 nM Hda was flowed over both the left and the right channels for 1.5 min at a flow rate of 25 μl/min. Kinetic constants were determined as described (25).

Biolayer interferometry experiments. BLI experiments were performed at 25°C using a FortéBio Octet Red 96e instrument (Sartorius). All interactions were analyzed in HBS-EP buffer (10 mM HEPES-KOH [pH 7.4], 150 mM NaCl, 3 mM EDTA, and 0.005% Tween 20) using FortéBio penta-His (HIS1K) Dip and Read biosensors. Biosensor tips were hydrated for 10 min in HBS-EP buffer and allowed to equilibrate in HBS-EP buffer for 1 min prior to loading N-terminally His_6- and heart muscle kinase-tagged ligand (1,000 nM β^+ or β^{E202K}). Following ligand capture, biosensors were quenched using SuperBlock (Thermo Scientific) and EZ-Link biocytin (50 μM; Thermo Fisher Scientific) for 5 min and then allowed to equilibrate for 3 min. The untagged analyte (50, 80, 110, and 140 nM Hda) was then allowed to associate with individual biosensors for 3 min in HBS-EP buffer supplemented with 10 mM magnesium acetate and 10 mM ADP, and dissociation was monitored for 3 min. Binding kinetics were then analyzed using FortéBio Data Analysis HT software (version 12.0.2.59; Molecular Devices LLC). Reference biosensors were also utilized to measure background and nonspecific binding.

Measurement of spontaneous Rif^r mutation frequency. Spontaneous Rif^r mutation frequencies were measured using saturated cultures inoculated from single colonies and grown at 37°C with aeration in LB medium. Fifteen cultures for each strain were serially diluted in 0.8% saline, and 100 μl of the 10^{-6} dilutions were sterilely spread on LB agar plates to measure colony formation. Cam was included for strains bearing pHSG576 or pHABcat. To measure the frequency of spontaneous mutations, 300 μl from 22 to 30 distinct cultures of each strain were spread on 150-mm LB agar plates supplemented with 50 μg/ml rifampin. Plates were incubated overnight (16 h) at 37°C. The spontaneous Rif^r mutation frequency of each strain was determined by dividing the number of CFU resistant to Rif by the average number of CFU measured in the absence of Rif. We calculated 95% confidence intervals using GraphPad Prism.

Data availability. The RNA-seq data discussed in this report have been deposited in NCBI's Gene Expression Omnibus (77) and are accessible through GEO Series accession number GSE175936.

ACKNOWLEDGMENTS

We thank Roel Schaaper (National Institute of Environmental Health Sciences) for plasmids pHSG576 and pHABcat, Phillip Page (Reichert Technologies, Life Sciences) for advice with kinetic analysis of SPR sensorgrams, Julia Grimwade (Florida Institute of Technology) for advice with flow cytometry, Daniel Kosman (University at Buffalo) for the use of his FLUOstar Omega microplate reader, Jessica Sutton for help with formatting the figures, and the members of our labs for helpful discussions.

Public Health Service awards R01 GM066094 (M.D.S.), R01 GM130761 (M.D.S.), R01 GM130761-02S1 (M.D.S.), and R01 GM090063 (J.M.K.) from the National Institutes of Health, NIGMS, supported this work. The funders had no role in study design, data collection or analysis, decision to publish, or the preparation of the manuscript.

We have no conflicts of interest to declare.

REFERENCES

1. Lopez de Saro F, Georgescu RE, Leu F, O'Donnell M. 2004. Protein trafficking on sliding clamps. Philos Trans R Soc Lond B Biol Sci 359:25–30. https://doi.org/10.1098/rstb.2003.1361.
2. Lopez de Saro FJ, O'Donnell M. 2001. Interaction of the beta sliding clamp with MutS, ligase, and DNA polymerase I. Proc Natl Acad Sci U S A 98:8376–8380. https://doi.org/10.1073/pnas.121009498.
3. Sutton MD. 2004. The Escherichia coli dnaN159 mutant displays altered DNA polymerase usage and chronic SOS induction. J Bacteriol 186:6738–6748. https://doi.org/10.1128/JB.186.20.6738-6748.2004.
4. Sutton MD. 2010. Coordinating DNA polymerase traffic during high and low fidelity synthesis. Biochim Biophys Acta 1804:1167–1179. https://doi.org/10.1016/j.bbapap.2009.06.010.
5. Kong XP, Onrust R, O'Donnell M, Kuriyan J. 1992. Three-dimensional structure of the beta subunit of *E. coli* DNA polymerase III holoenzyme: a sliding DNA clamp. Cell 69:425–437. https://doi.org/10.1016/0092-8674(92)90445-I.
6. Georgescu RE, Kim SS, Yurieva O, Kuriyan J, Kong XP, O'Donnell M. 2008. Structure of a sliding clamp on DNA. Cell 132:43–54. https://doi.org/10.1016/j.cell.2007.11.045.
7. Friedberg EC, Walker GC, Siede W, Wood RD, Schultz RA, Ellenberger T. 2006. DNA repair and mutagenesis, 2nd ed. American Society of Microbiology, Washington, DC. https://doi.org/10.1128/9781555816704.
8. Sutton MD, Opperman T, Walker GC. 1999. The *Escherichia coli* SOS mutagenesis proteins UmuD and UmuD' interact physically with the replicative DNA polymerase. Proc Natl Acad Sci U S A 96:12373–12378. https://doi.org/10.1073/pnas.96.22.12373.
9. Becherel OJ, Fuchs RP, Wagner J. 2002. Pivotal role of the beta-clamp in translesion DNA synthesis and mutagenesis in *E. coli* cells. DNA Repair (Amst) 1:703–708. https://doi.org/10.1016/S1568-7864(02)00106-4.
10. Ozaki S, Matsuda Y, Keyamura K, Kawakami H, Noguchi Y, Kasho K, Nagata K, Masuda T, Sakiyama Y, Katayama T. 2013. A replicase clamp-binding dynamin-like protein promotes colocalization of nascent DNA strands and equipartitioning of chromosomes in *E. coli*. Cell Rep 4:985–995. https://doi.org/10.1016/j.celrep.2013.07.040.
11. Kato J, Katayama T. 2001. Hda, a novel DnaA-related protein, regulates the replication cycle in *Escherichia coli*. EMBO J 20:4253–4262. https://doi.org/10.1093/emboj/20.15.4253.

Downloaded from https://journals.asm.org/journal/jb on 24 January 2022 by 35.10.240.139.

12. Pluciennik A, Burdett V, Lukianova O, O'Donnell M, Modrich P. 2009. Involvement of the beta clamp in methyl-directed mismatch repair *in vitro*. J Biol Chem 284:32782–32791. https://doi.org/10.1074/jbc.M109.054528.
13. Dalrymple BP, Kongsuwan K, Wijffels G, Dixon NE, Jennings PA. 2001. A universal protein-protein interaction motif in the eubacterial DNA replication and repair systems. Proc Natl Acad Sci U S A 98:11627–11632. https://doi.org/10.1073/pnas.191384398.
14. McHenry CS. 2011. Bacterial replicases and related polymerases. Curr Opin Chem Biol 15:587–594. https://doi.org/10.1016/j.cbpa.2011.07.018.
15. Kurth I, O'Donnell M. 2009. Replisome dynamics during chromosome duplication. EcoSal Plus 3. https://doi.org/10.1128/ecosalplus.4.4.2.
16. Dohrmann PR, McHenry CS. 2005. A bipartite polymerase-processivity factor interaction: only the internal beta binding site of the alpha subunit is required for processive replication by the DNA polymerase III holoenzyme. J Mol Biol 350:228–239. https://doi.org/10.1016/j.jmb.2005.04.065.
17. Jergic S, Horan NP, Elshenawy MM, Mason CE, Urathamakul T, Ozawa K, Robinson A, Goudsmits JM, Wang Y, Pan X, Beck JL, van Oijen AM, Huber T, Hamdan SM, Dixon NE. 2013. A direct proofreader-clamp interaction stabilizes the Pol III replicase in the polymerization mode. EMBO J 32:1322–1333. https://doi.org/10.1038/emboj.2012.347.
18. Toste Rego A, Holding AN, Kent H, Lamers MH. 2013. Architecture of the Pol III-clamp-exonuclease complex reveals key roles of the exonuclease subunit in processive DNA synthesis and repair. EMBO J 32:1334–1343. https://doi.org/10.1038/emboj.2013.68.
19. Fernandez-Leiro R, Conrad J, Scheres SH, Lamers MH. 2015. cryo-EM structures of the *E. coli* replicative DNA polymerase reveal its dynamic interactions with the DNA sliding clamp, exonuclease and tau. Elife 4:e11134. https://doi.org/10.7554/eLife.11134.
20. Naktinis V, Turner J, O'Donnell M. 1996. A molecular switch in a replication machine defined by an internal competition for protein rings. Cell 84:137–145. https://doi.org/10.1016/S0092-8674(00)81000-4.
21. Grigorian AV, Lustig RB, Guzman EC, Mahaffy JM, Zyskind JW. 2003. *Escherichia coli* cells with increased levels of DnaA and deficient in recombinational repair have decreased viability. J Bacteriol 185:630–644. https://doi.org/10.1128/JB.185.2.630-644.2003.
22. Babu VM, Sutton MD. 2014. A dnaN plasmid shuffle strain for rapid *in vivo* analysis of mutant *Escherichia coli* beta clamps provides insight into the role of clamp in *umuDC*-mediated cold sensitivity. PLoS One 9:e98791. https://doi.org/10.1371/journal.pone.0098791.
23. Sutton MD, Farrow MF, Burton BM, Walker GC. 2001. Genetic interactions between the *Escherichia coli umuDC* gene products and the beta processivity clamp of the replicative DNA polymerase. J Bacteriol 183:2897–2909. https://doi.org/10.1128/JB.183.9.2897-2909.2001.
24. Duzen JM, Walker GC, Sutton MD. 2004. Identification of specific amino acid residues in the *E. coli* beta processivity clamp involved in interactions with DNA polymerase III, UmuD and UmuD'. DNA Repair (Amst) 3:301–312. https://doi.org/10.1016/j.dnarep.2003.11.008.
25. Homiski C, Scotland MK, Babu VMP, Chodavarapu S, Maul RW, Kaguni JM, Sutton MD. 2021. The mutant β^{E202K} sliding clamp protein impairs DNA polymerase III replication activity. *J Bacteriol* https://doi.org/10.1128/JB.00303-21.
26. Sekimizu K, Bramhill D, Kornberg A. 1987. ATP activates dnaA protein in initiating replication of plasmids bearing the origin of the *E. coli* chromosome. Cell 50:259–265. https://doi.org/10.1016/0092-8674(87)90221-2.
27. Fuchs JA, Karlstrom HO. 1976. Mapping of *nrdA* and *nrdB* in *Escherichia coli* K-12. J Bacteriol 128:810–814. https://doi.org/10.1128/jb.128.3.810-814.1976.
28. Braun RE, O'Day K, Wright A. 1985. Autoregulation of the DNA replication gene *dnaA* in *E. coli* K-12. Cell 40:159–169. https://doi.org/10.1016/0092-8674(85)90319-8.
29. Wang QP, Kaguni JM. 1987. Transcriptional repression of the *dnaA* gene of *Escherichia coli* by dnaA protein. Mol Gen Genet 209:518–525. https://doi.org/10.1007/BF00331158.
30. Tesfa-Selase F, Drabble WT. 1992. Regulation of the *gua* operon of *Escherichia coli* by the DnaA protein. Mol Gen Genet 231:256–264. https://doi.org/10.1007/BF00279799.
31. Wang QP, Kaguni JM. 1989. dnaA protein regulates transcriptions of the *rpoH* gene of *Escherichia coli*. J Biol Chem 264:7338–7344. https://doi.org/10.1016/S0021-9258(18)83238-0.
32. Ogawa T, Okazaki T. 1994. Cell cycle-dependent transcription from the *gid* and *mioC* promoters of *Escherichia coli*. J Bacteriol 176:1609–1615. https://doi.org/10.1128/jb.176.6.1609-1615.1994.
33. Messer W, Weigel C. 1997. DnaA initiator–also a transcription factor. Mol Microbiol 24:1–6. https://doi.org/10.1046/j.1365-2958.1997.3171678.x.
34. Wurihan G, Brambilla E, Wang S, Sun H, Fan L, Shi Y, Sclavi BM. 2018. DnaA and LexA proteins regulate transcription of the *uvrB* gene in *Escherichia coli*: the role of DnaA in the control of the SOS regulon. Front Microbiol 9:1212. https://doi.org/10.3389/fmicb.2018.01212.
35. van den Berg EA, Geerse RH, Memelink J, Bovenberg RA, Magnee FA, van de Putte P. 1985. Analysis of regulatory sequences upstream of the *E. coli uvrB* gene; involvement of the DnaA protein. Nucleic Acids Res 13:1829–1840. https://doi.org/10.1093/nar/13.6.1829.
36. Ozaki T, Kumaki Y, Kitagawa R, Ogawa T. 2001. Anomalous DnaA protein binding to the regulatory region of the *Escherichia coli aldA* gene. Microbiology (Reading) 147:153–159. https://doi.org/10.1099/00221287-147-1-153.
37. Quinones A, Wandt G, Kleinstauber S, Messer W. 1997. DnaA protein stimulates *polA* gene expression in *Escherichia coli*. Mol Microbiol 23:1193–1202. https://doi.org/10.1046/j.1365-2958.1997.2961658.x.
38. Mizushima T, Koyanagi R, Katayama T, Miki T, Sekimizu K. 1997. Decrease in expression of the master operon of flagellin synthesis in a *dnaA46* mutant of *Escherichia coli*. Biol Pharm Bull 20:327–331. https://doi.org/10.1248/bpb.20.327.
39. Mizushima T, Tomura A, Shinpuku T, Miki T, Sekimizu K. 1994. Loss of flagellation in *dnaA* mutants of *Escherichia coli*. J Bacteriol 176:5544–5546. https://doi.org/10.1128/jb.176.17.5544-5546.1994.
40. Olliver A, Saggioro C, Herrick J, Sclavi B. 2010. DnaA-ATP acts as a molecular switch to control levels of ribonucleotide reductase expression in *Escherichia coli*. Mol Microbiol 76:1555–1571. https://doi.org/10.1111/j.1365-2958.2010.07185.x.
41. Limon A, Hidalgo E, Aguilar J. 1997. The *aldA* gene of *Escherichia coli* is under the control of at least three transcriptional regulators. Microbiology (Reading) 143(Pt 6):2085–2095. https://doi.org/10.1099/00221287-143-6-2085.
42. Pellicer MT, Lynch AS, De Wulf P, Boyd D, Aguilar J, Lin EC. 1999. A mutational study of the ArcA-P binding sequences in the *aldA* promoter of *Escherichia coli*. Mol Gen Genet 261:170–176. https://doi.org/10.1007/s004380050954.
43. Constantinidou C, Hobman JL, Griffiths L, Patel MD, Penn CW, Cole JA, Overton TW. 2006. A reassessment of the FNR regulon and transcriptomic analysis of the effects of nitrate, nitrite, NarXL, and NarQP as *Escherichia coli* K12 adapts from aerobic to anaerobic growth. J Biol Chem 281:4802–4815. https://doi.org/10.1074/jbc.M512312200.
44. Eppler T, Postma P, Schutz A, Volker U, Boos W. 2002. Glycerol-3-phosphate-induced catabolite repression in *Escherichia coli*. J Bacteriol 184:3044–3052. https://doi.org/10.1128/JB.184.11.3044-3052.2002.
45. Quintilla FX, Baldoma L, Badia J, Aguilar J. 1991. Aldehyde dehydrogenase induction by glutamate in *Escherichia coli*. Role of 2-oxoglutarate. Eur J Biochem 202:1321–1325. https://doi.org/10.1111/j.1432-1033.1991.tb16506.x.
46. Baxter JC, Sutton MD. 2012. Evidence for roles of the *Escherichia coli* Hda protein beyond regulatory inactivation of DnaA. Mol Microbiol 85:648–668. https://doi.org/10.1111/j.1365-2958.2012.08129.x.
47. Ortenberg R, Gon S, Porat A, Beckwith J. 2004. Interactions of glutaredoxins, ribonucleotide reductase, and components of the DNA replication system of *Escherichia coli*. Proc Natl Acad Sci U S A 101:7439–7444. https://doi.org/10.1073/pnas.0401965101.
48. Riber L, Olsson JA, Jensen RB, Skovgaard O, Dasgupta S, Marinus MG, Lobner-Olesen A. 2006. Hda-mediated inactivation of the DnaA protein and *dnaA* gene autoregulation act in concert to ensure homeostatic maintenance of the *Escherichia coli* chromosome. Genes Dev 20:2121–2134. https://doi.org/10.1101/gad.379506.
49. Keyamura K, Fujikawa N, Ishida T, Ozaki S, Su'etsugu M, Fujimitsu K, Kagawa W, Yokoyama S, Kurumizaka H, Katayama T. 2007. The interaction of DiaA and DnaA regulates the replication cycle in *E. coli* by directly promoting ATP DnaA-specific initiation complexes. Genes Dev 21:2083–2099. https://doi.org/10.1101/gad.1561207.
50. Fujimitsu K, Su'etsugu M, Yamaguchi Y, Mazda K, Fu N, Kawakami H, Katayama T. 2008. Modes of overinitiation, dnaA gene expression, and inhibition of cell division in a novel cold-sensitive *hda* mutant of *Escherichia coli*. J Bacteriol 190:5368–5381. https://doi.org/10.1128/JB.00044-08.
51. Babu VMP, Itsko M, Baxter JC, Schaaper RM, Sutton MD. 2017. Insufficient levels of the *nrdAB*-encoded ribonucleotide reductase underlie the severe growth defect of the Δ*hda E. coli* strain. Mol Microbiol 104:377–399. https://doi.org/10.1111/mmi.13632.
52. Toyotake Y, Nishiyama M, Yokoyama F, Ogawa T, Kawamoto J, Kurihara T. 2020. A novel lysophosphatidic acid acyltransferase of *Escherichia coli*

Downloaded from https://journals.asm.org/journal/jb on 24 January 2022 by 35.10.240.139.

produces membrane phospholipids with a cis-vaccenoyl group and is related to flagellar formation. Biomolecules 10:745. https://doi.org/10.3390/biom10050745.
53. Kren B, Fuchs JA. 1987. Characterization of the *ftsB* gene as an allele of the *nrdB* gene in *Escherichia coli*. J Bacteriol 169:14–18. https://doi.org/10.1128/jb.169.1.14-18.1987.
54. Fuchs JA, Karlstrom HO. 1973. A mutant of *Escherichia coli* defective in ribonucleosidediphosphate reductase. 2. Characterization of the enzymatic defect. Eur J Biochem 32:457–462.
55. Nazaretyan SA, Savic N, Sadek M, Hackert BJ, Courcelle J, Courcelle CT. 2018. Replication rapidly recovers and continues in the presence of hydroxyurea in *Escherichia coli*. J Bacteriol 200:e00713-17. https://doi.org/10.1128/JB.00713-17.
56. Chodavarapu S, Felczak MM, Simmons LA, Murillo A, Kaguni JM. 2013. Mutant DnaAs of *Escherichia coli* that are refractory to negative control. Nucleic Acids Res 41:10254–10267. https://doi.org/10.1093/nar/gkt774.
57. Kim JS, Nanfara MT, Chodavarapu S, Jin KS, Babu VMP, Ghazy MA, Chung S, Kaguni JM, Sutton MD, Cho Y. 2017. Dynamic assembly of Hda and the sliding clamp in the regulation of replication licensing. Nucleic Acids Res 45:3888–3905. https://doi.org/10.1093/nar/gkx081.
58. Su'etsugu M, Nakamura K, Keyamura K, Kudo Y, Katayama T. 2008. Hda monomerization by ADP binding promotes replicase clamp-mediated DnaA-ATP hydrolysis. J Biol Chem 283:36118–36131. https://doi.org/10.1074/jbc.M803158200.
59. Herrick J, Sclavi B. 2007. Ribonucleotide reductase and the regulation of DNA replication: an old story and an ancient heritage. Mol Microbiol 63:22–34. https://doi.org/10.1111/j.1365-2958.2006.05493.x.
60. Gon S, Napolitano R, Rocha W, Coulon S, Fuchs RP. 2011. Increase in dNTP pool size during the DNA damage response plays a key role in spontaneous and induced-mutagenesis in Escherichia coli. Proc Natl Acad Sci U S A 108:19311–19316. https://doi.org/10.1073/pnas.1113664108.
61. Gon S, Camara JE, Klungsoyr HK, Crooke E, Skarstad K, Beckwith J. 2006. A novel regulatory mechanism couples deoxyribonucleotide synthesis and DNA replication in *Escherichia coli*. EMBO J 25:1137–1147. https://doi.org/10.1038/sj.emboj.7600990.
62. Augustin LB, Jacobson BA, Fuchs JA. 1994. *Escherichia coli* Fis and DnaA proteins bind specifically to the *nrd* promoter region and affect expression of an *nrd-lac* fusion. J Bacteriol 176:378–387. https://doi.org/10.1128/jb.176.2.378-387.1994.
63. Park MS, O'Donnell M. 2009. The clamp loader assembles the beta clamp onto either a 3' or 5' primer terminus: the underlying basis favoring 3' loading. J Biol Chem 284:31473–31483. https://doi.org/10.1074/jbc.M109.050310.
64. Garibyan L, Huang T, Kim M, Wolff E, Nguyen A, Nguyen T, Diep A, Hu K, Iverson A, Yang H, Miller JH. 2003. Use of the *rpoB* gene to determine the specificity of base substitution mutations on the *Escherichia coli* chromosome. DNA Repair (Amst) 2:593–608. https://doi.org/10.1016/s1568-7864(03)00024-7.
65. Wijffels G, Dalrymple BP, Prosselkov P, Kongsuwan K, Epa VC, Lilley PE, Jergic S, Buchardt J, Brown SE, Alewood PF, Jennings PA, Dixon NE. 2004. Inhibition of protein interactions with the beta 2 sliding clamp of *Escherichia coli* DNA polymerase III by peptides from beta 2-binding proteins. Biochemistry 43:5661–5671. https://doi.org/10.1021/bi036229j.
66. Katayama T, Kubota T, Kurokawa K, Crooke E, Sekimizu K. 1998. The initiator function of DnaA protein is negatively regulated by the sliding clamp of the *E. coli* chromosomal replicase. Cell 94:61–71. https://doi.org/10.1016/S0092-8674(00)81222-2.
67. Kawakami H, Su'etsugu M, Katayama T. 2006. An isolated Hda-clamp complex is functional in the regulatory inactivation of DnaA and DNA replication. J Struct Biol 156:220–229. https://doi.org/10.1016/j.jsb.2006.02.007.
68. Su'etsugu M, Shimuta TR, Ishida T, Kawakami H, Katayama T. 2005. Protein associations in DnaA-ATP hydrolysis mediated by the Hda-replicase clamp complex. J Biol Chem 280:6528–6536. https://doi.org/10.1074/jbc.M412060200.
69. Soufo CD, Soufo HJ, Noirot-Gros MF, Steindorf A, Noirot P, Graumann PL. 2008. Cell-cycle-dependent spatial sequestration of the DnaA replication initiator protein in *Bacillus subtilis*. Dev Cell 15:935–941. https://doi.org/10.1016/j.devcel.2008.09.010.
70. Banach-Orlowska M, Fijalkowska IJ, Schaaper RM, Jonczyk P. 2005. DNA polymerase II as a fidelity factor in chromosomal DNA synthesis in *Escherichia coli*. Mol Microbiol 58:61–70. https://doi.org/10.1111/j.1365-2958.2005.04805.x.
71. Kaguni JM, Kornberg A. 1984. Replication initiated at the origin (*oriC*) of the *E. coli* chromosome reconstituted with purified enzymes. Cell 38:183–190. https://doi.org/10.1016/0092-8674(84)90539-7.
72. Kaguni J, LaVerne LS, Ray DS. 1979. Cloning and expression of the *Escherichia coli* replication origin in a single-stranded DNA phage. Proc Natl Acad Sci U S A 76:6250–6254. https://doi.org/10.1073/pnas.76.12.6250.
73. Heltzel JM, Maul RW, Scouten Ponticelli SK, Sutton MD. 2009. A model for DNA polymerase switching involving a single cleft and the rim of the sliding clamp. Proc Natl Acad Sci U S A 106:12664–12669. https://doi.org/10.1073/pnas.0903460106.
74. Maul RW, Ponticelli SK, Duzen JM, Sutton MD. 2007. Differential binding of *Escherichia coli* DNA polymerases to the beta-sliding clamp. Mol Microbiol 65:811–827. https://doi.org/10.1111/j.1365-2958.2007.05828.x.
75. Bradford MM. 1976. A rapid and sensitive method for the quantitation of microgram quantities of protein utilizing the principle of protein-dye binding. Anal Biochem 72:248–254. https://doi.org/10.1006/abio.1976.9999.
76. Scouten Ponticelli SK, Duzen JM, Sutton MD. 2009. Contributions of the individual hydrophobic clefts of the *Escherichia coli* beta sliding clamp to clamp loading, DNA replication and clamp recycling. Nucleic Acids Res 37:2796–2809. https://doi.org/10.1093/nar/gkp128.
77. Edgar R, Domrachev M, Lash AE. 2002. Gene Expression Omnibus: NCBI gene expression and hybridization array data repository. Nucleic Acids Res 30:207–210. https://doi.org/10.1093/nar/30.1.207.
78. Wang RF, Kushner SR. 1991. Construction of versatile low-copy-number vectors for cloning, sequencing and gene expression in Escherichia coli. Gene 100:195–199. https://doi.org/10.1016/0378-1119(91)90366-J.
79. Maul RW, Sutton MD. 2005. Roles of the *Escherichia coli* RecA protein and the global SOS response in effecting DNA polymerase selection in vivo. J Bacteriol 187:7607–7618. https://doi.org/10.1128/JB.187.22.7607-7618.2005.
80. Takeshita S, Sato M, Toba M, Masahashi W, Hashimoto-Gotoh T. 1987. High-copy-number and low-copy-number plasmid vectors for *lacZ* alpha-complementation and chloramphenicol- or kanamycin-resistance selection. Gene 61:63–74. https://doi.org/10.1016/0378-1119(87)90365-9.
81. Ahluwalia D, Bienstock RJ, Schaaper RM. 2012. Novel mutator mutants of *E. coli nrdAB* ribonucleotide reductase: insight into allosteric regulation and control of mutation rates. DNA Repair (Amst) 11:480–487. https://doi.org/10.1016/j.dnarep.2012.02.001.
82. Hwang DS, Kaguni JM. 1988. Purification and characterization of the *dnaA46* gene product. J Biol Chem 263:10625–10632.

Downloaded from https://journals.asm.org/journal/jb on 24 January 2022 by 35.10.240.139.